A non-DNA-binding activity for the ATHB4 transcription factor in the control of vegetation proximity

Marçal Gallemí[1], Maria Jose Molina-Contreras[1*], Sandi Paulišić[1*], Mercè Salla-Martret[1], Céline Sorin[1], Marta Godoy[2], Jose Manuel Franco-Zorrilla[2], Roberto Solano[2], Jaime F. Martínez-García[1,3]©

[1] Centre for Research in Agricultural Genomics (CRAG), CSIC-IRTA-UAB-UB, Campus UAB, Bellaterra, 08193-Barcelona, Spain; [2] National Centre for Biotechnology (CNB), CSIC, Campus University Autónoma, 28049-Madrid, Spain; [3] Institució Catalana de Recerca i Estudis Avançats (ICREA), 08010-Barcelona, Spain.

*, these authors contributed equally to this work.

©Author for correspondence,

Tel: +34 935 636 600, ext 3216

E-mail: jaume.martinez@cragenomica.es

The main body of the text (excluding references and figure legends) has 6422 words.

Word counting for each section: Introduction (807), Materials and Methods (651), Results (3196), Discussion (1768) and Acknowledgements (180).

This manuscript has 9 figures (all in color). Supporting information has 9 figures and 4 Tables.

Short title: Non-DNA binding activity of ATHB4

Twiter accounts: @RosPlanelles, @CRAGENOMICA.

SUMMARY

● In plants, perception of vegetation proximity by phytochrome photoreceptors activate a transcriptional network that implements a set of responses to adapt to plant competition, including elongation of stems or hypocotyls. In *Arabidopsis thaliana*, the homeodomain-leucine zipper (HD-Zip) transcription factor ATHB4 regulates this and other responses, such as leaf polarity.

● To better understand the shade regulatory transcriptional network, we have carried out structure-function analyses of ATHB4 by overexpressing a series of truncated and mutated forms and analyzing three different responses: hypocotyl response to shade, transcriptional activity and leaf polarity.

● Our results indicated that ATHB4 has two physically separated molecular activities: the HD-Zip, involved in binding to DNA-regulatory elements, and the ERF-associated amphiphilic repression- (EAR-) containing N-terminal region, involved in protein-protein interaction. Whereas both activities are required to regulate leaf polarity, DNA-binding activity is not required for the regulation of the seedling responses to plant proximity, which indicates that ATHB4 works as a transcriptional co-factor in the regulation of this response.

● These findings suggest that transcription factors might employ alternative mechanisms of action to regulate different developmental processes.

Keywords: Arabidopsis; ATHB4; DNA-binding activity; EAR motif; Homeodomain-leucine zipper; Shade avoidance syndrome; Transcription factors; Transcriptional cofactors.

INTRODUCTION

Transcriptional control is at the base of how living organisms develop and adapt to their surroundings. In plants, deciphering transcriptional mechanisms that control gene expression is fundamental for understanding development plasticity. In crowded vegetation, light for photosynthesis might become limiting: in various species, growing in high plant density environment activates the shade avoidance syndrome (SAS), a set of strategic responses to adjust growth that has a strong impact on plant development. SAS includes modulation of hypocotyl and stem elongation, leaf expansion, flowering time or levels of photosynthetic pigments. Plant proximity or shade is perceived as a light signal: the surrounding canopy, which absorbs the red light (R) and reflects the far red light (FR), reduces the R to FR ratio (R:FR), a signal perceived by the phytochrome photoreceptors. Phytochromes exist in two photoconvertible forms, an inactive R-absorbing Pr form and an active FR-absorbing Pfr form. In fully de-etiolated plants, high R:FR displaces the photo-equilibrium towards the active Pfr, whereas the low R:FR signal from crowded vegetation displaces the photo-equilibrium towards the inactive Pr. Mechanistically, the interaction of active phytochromes with PHYTOCHROME INTERACTING FACTORs (PIFs), transcriptional regulators of the basic helix–loop–helix (bHLH) family, modulates the expression of *PHYTOCHROME RAPIDLY REGULATED* (*PAR*) genes. Shade induced changes in *PAR* expression eventually activates the SAS (Martinez-Garcia *et al.*, 2010; Leivar & Quail, 2011; Casal, 2013; Bou-Torrent *et al.*, 2015).

Molecular analyses revealed that PIFs positively regulate some *PAR* genes expressed during the shade-induced hypocotyl elongation, such as *ATHB2*, *HFR1* and *PIL1* (Lorrain *et al.*, 2008; Li *et al.*, 2012). Genetic analyses have also involved a diversity of non-PIF factors in the regulation of SAS hypocotyl response that, nonetheless, also participate in the modulation of *PAR* gene expression, such as HD-Zip class III, CONSTITUTIVE SHADE AVOIDANCE 1 and DRACULA2 (a nucleopore complex component) (Faigon-Soverna *et al.*, 2006; Brandt *et al.*, 2012; Gallemi *et al.*, 2016), highlighting the complexity of the transcriptional network that implements the SAS responses. Further genetic studies of this response

demonstrated roles for several *PAR* genes encoding transcriptional regulators of at least 3 different families: homedomain-leucine zipper (HD-Zip) class II (*ATHB2*, *ATHB4*, *HAT1*, *HAT2* and *HAT3*), B-BOX CONTAINING (BBX) and bHLH (e.g., *BEEs*, *BIMs*, *HFR1*, *PAR1*, *PAR2* and *PIL1*). BBX and bHLH members appear to have negative (HFR1, PAR1, PIL1, BBX21 and BBX22) and positive (BEEs, BIMs, BBX24, BBX25, ATHB2, HAT1, HAT2 and HAT3) roles (Steindler *et al.*, 1999; Sessa *et al.*, 2005; Roig-Villanova *et al.*, 2007; Sorin *et al.*, 2009; Crocco *et al.*, 2010; Hornitschek *et al.*, 2012; Cifuentes-Esquivel *et al.*, 2013; Crocco *et al.*, 2015; Turchi *et al.*, 2015). In the case of the identified members of the HD-Zip II family, their overexpression results in a phenotype in high R:FR that is reminiscent of that displayed by wild-type plants grown in low R:FR, and hence these factors have been proposed as SAS positive regulators (Ciarbelli *et al.*, 2008; Turchi *et al.*, 2015). A deeper analyses of ATHB4 activity, however, indicated an attenuated hypocotyl elongation in both loss- and gain-of-function mutants grown under low R:FR, which led to propose that ATHB4, rather than positive, is a SAS complex regulator (Sorin *et al.*, 2009).

Proteins of the HD-Zip family have a HD adjacent to the Zip motif, an association that is unique to plants. The HD is responsible for the specific binding to DNA, whereas the Zip acts as a dimerization motif: HD-Zip proteins bind to DNA as dimers and recognize pseudo-palindromic *cis* elements; the absence of the Zip absolutely abolishes their DNA-binding ability (Ariel *et al.*, 2007). Overexpression of HD-Zip II transcription factors (TFs) has provided evidence that several of them function as negative regulators of gene expression (Steindler *et al.*, 1999; Ohgishi *et al.*, 2001; Sawa *et al.*, 2002; Sorin *et al.*, 2009) in contrast with other HD-Zip proteins, e.g. those of subfamily III (Brandt *et al.*, 2012; Turchi *et al.*, 2013; Xie *et al.*, 2015), that act as transcriptional activators. Several of the HD-Zip II proteins contain in their conserved N-terminal region an ERF-associated amphiphilic repression (EAR) motif, which might be involved in the transcriptional repressor activity (Brandt *et al.*, 2014).

To understand how complex transcriptional networks control a process, in addition to identify the components and their organization into functional modules,

it is basic to clarify the basic mechanism of transcriptional control of the individual components. In this paper we aim to address this latter aspect of ATHB4, a complex SAS regulatory component whose molecular and biological activity is not well understood (Sorin *et al.*, 2009) and that emerges as a paradigm to understand other HD-Zip II members. After analyzing its DNA-binding and transcriptional properties, we performed a detailed structure-function analysis of ATHB4 activity by overexpressing truncated and mutated derivatives in Arabidopsis. As a result, we could establish the mechanistic duality of this transcriptional regulator in modulating different environmental and developmental responses.

MATERIAL AND METHODS

Plant material and growth conditions

Arabidopsis thaliana (Arabidopsis) plants were grown in the greenhouse to produce seeds. Line overexpressing *ATHB4* fused to *GR* (35S:ATHB4-GR.05) (Sorin *et al.*, 2009) and the new transgenic lines presented in this work were all in the Col-0 background. Experiments were performed with surface-sterilized seeds sown on Petri dishes containing solid growth medium without sucrose (0.5xGM–) (Roig-Villanova *et al.*, 2006), unless otherwise stated. For gene expression and chromatin immunoprecipitation (ChIP) analyses seeds were sown on filter paper or nylon membranes placed on top of the 0.5xGM–. After stratification (3–5 days) plates were incubated in a growth chamber at 22ºC under W, that was provided by four cool-white vertical fluorescent tubes (25 $\mu mol \cdot m^{-2} \cdot s^{-1}$ of photosynthetically active radiation; R:FR ratio of 2.8-6.3). Simulated shade (W+FR) was generated by enriching W with supplementary FR provided by GreenPower LED module HF far-red (Philips, www.philips.com/horti) (25 $\mu mol \cdot m^{-2} \cdot s^{-1}$ of photosynthetically active radiation; R:FR ratio of 0.06). Fluence rates were measured using a Spectrosense2 meter associated with a 4-channel sensor (Skye Instruments Ltd., www.skyeinstruments.com) (Martinez-Garcia *et al.*, 2014).

Measurement of hypocotyl length

The National Institutes of Health ImageJ software (Bethesda, MD, USA; http://rsb.info.nih.gov/) was used on digital images to measure hypocotyl length as indicated (Sorin *et al.*, 2009). At least 15 seedlings were used for each treatment and experiments were repeated 3–5 times and a representative one is shown. Statistical analyses of the data (t-test and two-way ANOVA) were performed using GraphPad Prism version 4.00 for Windows (http://www.graphpad.com/).

Construction of transgenic lines

Details of the generation of the described transgenic lines are given in Methods S1. Sequences of the primer used can be found in the Table S1. For each construct, more than ten independent transgenic lines were identified; from those, at least two independent transgenic lines showing detectable levels of transgene expression were selected and characterized, although only a representative one is shown.

Gene expression analysis

For microarray analysis, plant material was prepared and analyzed as indicated in Methods S2. For real-time qPCR analysis, triplicate samples were harvested. Total RNA was isolated from seedlings or adult leaves using commercial kits (RNAeasy Plant Mini kit, Qiagen, www.qiagen.com; or the semi-automatic Maxwell SimplyRNA kit, Promega, www.promega.com). Two micrograms of RNA were reverse-transcribed using the M-MLV Reverse Transcriptase (Invitrogen, www.lifetechnologies.com) or Transcriptor First Strand cDNA synthesis (Roche, lifescience.roche.com) and qPCR analyses of gene expression were performed as indicated elsewhere (Cifuentes-Esquivel *et al.*, 2013). The *UBQ10* gene was used as a control for normalizations. Primer sequences can be found in the Table S2. Details of RNA bolt analyses are given in Methods S3.

Yeast Two Hybrid (Y2H) assays

Details of the Y2H screening and directed assays, and the constructs used are given in Methods S4.

Subcellular localization analyses

Confocal microscopy was performed in bombarded onion epidermal cells or agroinfiltrated *N. benthamiana* leaves using either a Leica TCS SP5 II or an Olympus FV1000.2.4 confocal microscope. Details of the constructs and the protocols used for the bombardments or the agroinfiltration are given in Methods S5.

Expression of recombinant ATHB4-MBP.

Details of the constructs and protocols used for the production of the recombinant ATHB4-MBP for the Protein Binding Microarrays (PBMs) are given in Methods S6.

Chromatin immunoprecipitation (ChIP) and protein immunodetection analyses.

Details of the protocol of the ChIP assay, lines used and promoters analyzed are given in Methods S7. Details of protein extraction and immunoblot analyses are given in Methods S8.

Chemical treatments

Cycloheximide (CHX, Sigma-Aldrich) was dissolved at 50 mM in 50% (v/v) ethanol. Dexamethasone (DEX, Sigma-Aldrich) was dissolved in absolute ethanol at 50 mM. Stock solutions were kept at –20ºC until use.

Accession numbers

Sequence data from this paper can be found in the Arabidopsis Genome Initiative or GenBank/EMBL databases under the following accession numbers: *ATHB2* (At4g16780), *ATHB4* (At2g44910), *HAT2* (At5g47370) and *SAUR15* (At4g38850). The full data set is available to download from the NASCarrays database (affymetrix.Arabidopsis.info; reference: NASCARRAYS-545).

RESULTS

Overexpression of HD-Zip II members similarly alters hypocotyl responses to simulated shade

First, we aimed to address whether overexpression of other HD-Zip II members affected hypocotyl elongation in response to simulated shade (W+FR) as *ATHB4*. We used available lines constitutively expressing *ATHB2* (35S:ATHB2) and *HAT2* (35S:HAT2) (Ciarbelli *et al.*, 2008), and newly prepared transgenic lines constitutively expressing *HAT1* (35S:HAT1) and *ATHB4-GFP* (35S:ATHB4-GFP) (Methods S1). Non-transformed (Col-0) plants were used as controls. Under continuous white light (W), constitutive overexpression of these HD-Zip II members promoted hypocotyl elongation compared to wild-type seedlings, as expected. By contrast, under W+FR hypocotyl length was inhibited in 35S:HAT1 and 35S:ATHB4-GFP seedlings and unaffected in 35S:ATHB2 and 35S:HAT2 seedlings (Figure S1A-D). These analyses indicate that constitutive overexpression of HD-Zip II members promotes hypocotyl elongation under W, whereas it had no effect or even inhibited this trait under simulated shade.

We next used an inducible transgenic line constitutively expressing a fusion between *ATHB4* and the *GR* domain of the rat glucocorticoid receptor, which encodes the hormone-binding domain (35S:ATHB4-GR line) (Sorin *et al.*, 2009). In the absence of glucocorticoids, the resulting protein is retained in the cytoplasm; upon the addition of the synthetic glucocorticoid dexamethasone (DEX), the fusion protein translocates to the nucleus, where it acts. When using this transgenic line, increasing concentrations of DEX resulted in a progressive reduction of the hypocotyl length under W+FR, whereas it did not affect it under W (Figure S1E), an effect not observed in Col-0 seedlings. When using inducible transgenic 35S:HAT2-GR lines, DEX-induced HAT2 was also shown to strongly inhibit hypocotyl elongation under W+FR and to be ineffective in promoting hypocotyl elongation under W (Figure S1F). These results showed that different HD-Zip II members (1) inhibit hypocotyl elongation under simulated shade; (2) promote hypocotyl elongation under W only when constitutively expressed; and (3) this latter promoting activity is absent in the GR-fusions even when DEX is applied. Together, our results indicate that HD-Zip II proteins only promote hypocotyl

elongation under limited conditions, and therefore argue against considering them as SAS positive regulators.

ATHB4 acts fundamentally as a transcriptional repressor

To obtain a deeper understanding of ATHB4 function, we identified its target genes on a genome-wide scale using the 35S:ATHB4-GR line (Sorin *et al.*, 2009). To establish (1) a list of putative direct targets of ATHB4 activity, and (2) whether this HD-Zip II regulator acts as a repressor or an activator of gene expression, we performed triplicate microarray experiments (Affymetrix microarray platform; see Methods S2 for a full description) using the 35S:ATHB4-GR line. Transgenic seedlings grown for 7 days under W were treated during 4 hours with or without DEX in the absence or presence of the protein synthesis inhibitor cycloheximide (±CHX) (i.e., a total of four treatments; Figure 1A). In the absence of CHX (–CHX), addition of DEX altered the expression of 433 genes ($\geq$ 1.5-fold), whereas in the presence of CHX (+CHX), addition of DEX altered the expression of 1055 genes (Figure 1B; Table S3). Comparison of the DEX-regulated genes in absence and presence of CHX highlighted 104 ATHB4-regulated genes whose expression does not require *de novo* protein synthesis, likely reflecting direct targets of ATHB4 action. Among these 104 genes were found *HAT1*, *HAT2* and *HAT22* (Figure 1B; Table S3), previously shown as repressed by ATHB4 (Sorin *et al.*, 2009). Although *ATHB2* was not found in this list, it is directly repressed by ATHB2 itself, HAT2 and the ATHB4 paralog HAT3 (Ohgishi *et al.*, 2001; Sawa *et al.*, 2002; Turchi *et al.*, 2013), which suggested that it is also directly regulated by ATHB4 (see below). From this list of 104 genes, 97 were repressed by DEX application (i.e., by ATHB4) and only 7 up-regulated (Figure 1B), supporting that ATHB4 acts fundamentally as a transcriptional repressor of gene expression.

ATHB4 binds to specific DNA sequences

To test the ability of ATHB4 to specifically bind DNA, we next hybridized Protein-binding microarrays (PBMs) using recombinant ATHB4-MBP protein (produced as a fusion to the Maltose Binding Protein; Methods S6) (Godoy *et al.*,

2011). ATHB4 showed a strong preference for the 7-mer pseudopalindromic AAT(G/C)ATT sequence; binding of ATHB4 preferred the nucleotide A immediately 5' and 3' of this core sequence, resulting in the 9-mer consensus AAAT(G/C)ATTA sequence (Figure 1C). Binding of ATHB4 to the 7-mer core sequence *in vitro* was poorly influenced by the central G/C nucleotides, in position 4, and strongly influenced by the nucleotides A and T, in positions 2 and 6 respectively (Figure 1D). These results demonstrated that ATHB4 does possess a sequence specific DNA-binding capacity that is similar to that shown for its close relatives HAT3 and ATHB2 (NAAT(G/C)ATTN) (Turchi *et al.*, 2013). Combining the target sequence information with co-expression analyses allows predicting whether specific TFs act as activators or repressors through a particular DNA sequence (Franco-Zorrilla *et al.*, 2014). A similar analysis for ATHB4 target sequence specificity showed that the promoters of negatively co-regulated genes were enriched in binding motifs for ATHB4 (Figure S2), in agreement with our conclusion that ATHB4 acts mainly as a transcriptional repressor.

Apart from the HD and Zip domains, members of the HD-Zip class II show a high conservation in two additional regions: the C-terminal end, which contains the five conserved amino acids CPSCE sequence (proposed as responsible for sensing the redox cell state), and an N-terminal consensus sequence, of unknown function (Ariel *et al.*, 2007). Aligning the amino acid sequences of ATHB4 and ATHB2, which has been studied in some detail (Sessa *et al.*, 1997), led to divide ATHB4 into four regions: N-terminal (N, 1-142), HD (H, 143-219), Zip (Z, 220-263) and C-terminal (C, 264-318) (Figure S3A). Using a yeast two-hybrid (Y2H) assay, we observed that the HZ region of ATHB4 interacts with itself (Figure S3B-C), in agreement with the view that ATHB4 dimerizes via the Zip motif to bind to the DNA.

The HD region contains a functional Nuclear Localization Signal (NLS)

Next, seven truncated constructs were generated (NHZ0, 0HZ0, 00Z0, 00ZC, 0HZC, NH00 and 0H00), fused to the *GFP* reporter gene and placed under the control of the constitutive 35S promoter to study their subcellular localization *in*

vivo in onion epidermal cells by microbombardment assays. Full-length ATHB4 fused to GFP (35S:ATHB4-GFP) and GFP alone (35S:GFP) constructs were used as controls. The individual constructs were cotransformed with a plasmid to constitutively express the DsRed protein (a Red Fluorescent Protein, RFP), to identify the transformed cells. As expected, cytoplasmic and nuclear localization were observed for the GFP alone, whereas full-length ATHB4-GFP was mostly nuclear (Figure S4A-B). Variants containing the HD region (NHZ0, 0HZ0, 0HZC, NH00 and 00H0) displayed GFP fluorescence quite restricted to the nuclei, whereas the rest (00Z0 and 00ZC) showed a GFP fluorescence pattern similar to the one of the GFP alone (Figure S4C-I). These results suggested that the HD contains a nuclear localization signal (NLS). Indeed, a web-based program (http://nls-mapper.iab.keio.ac.jp/), predicted the existence of a monopartite NLS (GDGS**RKK**L**R**LS) within the HD, which is conserved in the HD of other members of the HD-Zip II family (Figure S4J).

The DNA-binding activity of ATHB4 is not required for controlling seedling responses to simulated shade

Next, we aimed to address the function of the different regions of ATHB4 in transgenic plants. From the possible genetic backgrounds to get transgenics, we chose to transform wild-type plants rather than the double *athb4 hat3* mutant for two main reasons. On one hand, the latter genotype displays an important set of developmental defects at both vegetative (leaf and cotyledon polarity defects) and reproductive stages (severe flower structure alteration, and very low fertility) (Bou-Torrent *et al.*, 2012; Reymond *et al.*, 2012; Turchi *et al.*, 2013) that might prevent plant transformation. More importantly, because the defective cotyledons of the *athb4 hat3* seedlings might affect the hypocotyl response to shade by indirect mechanisms (Sorin *et al.*, 2009), the possible complementation of the cotyledon and leaf defects by some ATHB4 derivatives might also interfere with the hypocotyl elongation response, preventing an adequate interpretation of the results. On the other hand, overexpression of *ATHB4* derivatives in a wild-type background provides morphological and molecular phenotypes that can be easily compared

with those of the full-length wild-type ATHB4 form (see below). Therefore, to analyze the structure-function relationship of ATHB4, we overexpressed the truncated *ATHB4* forms fused to the *GR* domain in wild-type plants (Figure 2A).

Non-transformed (Col-0) and transgenic 35S:ATHB4-GR plants (Sorin *et al.*, 2009) were used as controls. DEX application had little effect on Col-0 whereas it inhibited general growth in transgenic 35S:ATHB4-GR seedlings grown either under W or W+FR (Figures S5A-B), in agreement with published information (Sorin *et al.*, 2009). ATHB4 biological activity was easily scored by comparing the simulated shade induced hypocotyl length of seedlings grown in media supplemented with or without DEX (Figure S5C). Therefore, in the following experiments, the biological activity of ATHB4 derivatives was estimated as the ratio of hypocotyl length of W+FR-grown seedlings in the presence and absence of DEX (Figures 2B, S5D). Amongst the different lines generated, only seedlings overexpressing *NHZ0-GR*, *00ZC-GR*, *0HZC-GR* and *NH00-GR* displayed a significant DEX-dependent attenuated response to W+FR, similar to 35S:ATHB4-GR seedlings (Figure 2C). Independently on the hypocotyl phenotype, all the analyzed lines had detectable levels of transgene expression (Figure S6). These results suggest that both the C-terminal region and, surprisingly, the DNA-binding activity of ATHB4 are dispensable for the modulation of the seedling responses to simulated shade.

Next, we molecularly characterized those lines that showed different degrees of biological activity (35S:NHZ0-GR, 35S:00ZC-GR, 35S:0HZC-GR and 35S:NH00-GR). The DEX effect on the expression of the shade-marker genes *HAT2*, *SAUR15* (identified previously as putative direct targets of ATHB4 action, Table S3) and *ATHB2* was investigated. As controls we used 35S:ATHB4-GR and 35S:0HZ0-GR seedlings, which show full and no biological activity in the inhibition of shade-induced hypocotyl elongation, respectively. To better visualize the DEX-dependent repressor effect of ATHB4 over gene expression, seedlings were treated with W+FR for 1 h, which induces the expression of these genes, before harvesting the material (Figure 3A). *HAT2*, *SAUR15* and *ATHB2* expression was reduced in DEX-treated 35S:ATHB4-GR and 35S:NHZ0-GR seedlings (+DEX)

compared to those grown in the absence of DEX (-DEX), whereas it was unaffected in wild-type (Col-0) seedlings. Surprisingly, 35S:0HZ0-GR seedlings also presented a slight but significant DEX-dependent up-regulation of *ATHB2* expression, whereas *HAT2* and *SAUR15* expression was unaffected. *HAT2* expression was down-regulated only in DEX-treated 35S:NH00-GR seedlings whereas *SAUR15* was down-regulated in DEX-treated 35S:00ZC-GR and 35S:NH00-GR seedlings. By contrast *ATHB2* expression was unaffected in DEX-treated 35S:00ZC-GR and 35S:NH00-GR seedlings and slightly but significantly up-regulated in 35S:0HZC-GR seedlings (Figures 3B-E). Despite the complexity of the observed expression profiles, our results clearly show that to repress gene expression neither the DNA-binding activity of ATHB4 nor the protein dimerization via the Zip domain are required.

To deepen into this observation, a derivative of ATHB4 with an impaired DNA-binding was generated by mutating the Asn210, located in the HD, into an Ala ($ATHB4_{N210A}$) (Figure 4A). This residue was selected because of the reported effect of the equivalent mutation on the DNA-binding activity of ATHB2 ($ATHB2_{N176A}$) (Sessa *et al.*, 1997). Protein-binding microarrays (PBM) indicated that $ATHB4_{N210A}$ had no binding preference for any DNA sequence (Figure 4B, S7A-D), confirming that it was unable to bind specifically DNA. Seedlings overexpressing this mutant form fused to the *GR* (35S:$ATHB4_{N210A}$-GR) displayed a significant DEX-dependent attenuated hypocotyl elongation in response to W+FR, similar to 35S:ATHB4-GR seedlings (Figures 4C, S7E-F). Molecularly, the effect of DEX on the expression of *HAT2*, *SAUR15* and *ATHB2* genes mirrored that observed in 35S:NH00-GR seedlings (Figure 4E). Together these results confirm that DNA-binding activity is neither necessary nor sufficient for the modulation of the shade-induced hypocotyl elongation or for the control of gene expression by ATHB4 (at least for *HAT2* and *SAUR15*). These results also indicate that *ATHB2* expression is only affected by the DNA-binding activity of ATHB4 (Figures 3, 4E).

To address whether the analyzed genes are direct targets of the non-DNA-binding ATHB4 derivatives, we followed the strategy used to identify putative direct

targets of full-length ATHB4 activity (see Figure 1A) using 35S:NH00-GR and 35S:ATHB4$_{N210A}$-GR lines. As controls we employed Col-0 and 35S:ATHB4-GR lines. As in Figure 1A, seedlings were grown and treated with or without DEX in the absence or presence of the protein synthesis inhibitor cycloheximide (±CHX) during 4 hours. As in Figure 3, seedlings were treated with 1h of W+FR before harvesting the samples (Figure 5A). In Col-0 and 35S:NH00-GR seedlings, addition of DEX had no significant effect on the expression of *HAT2*, *SAUR15* and *ATHB2* independently on the presence of CHX. In 35S:ATHB4-GR seedlings, *HAT2*, *SAUR15* and *ATHB2* expression was reduced by DEX application in the absence of CHX (–CHX); by contrast, only *SAUR15* expression was also repressed by DEX in +CHX seedlings, further supporting our previous conclusion that *SAUR15* is a direct target of ATHB4. In 35S:ATHB4$_{N210A}$-GR seedlings, *HAT2* and *SAUR15* expression was reduced by DEX in –CHX samples, although only *SAUR15* expression was also repressed by DEX in +CHX seedlings; by contrast *ATHB2* expression was promoted by DEX in both –CHX and +CHX samples (Figure 5B). These results indicate an attenuated direct transcriptional activity of the truncated NH00 compared to the mutant ATHB4$_{N210A}$ derivative. In addition, they also suggest that *SAUR15* and *ATHB2* are direct targets of the non-DNA-binding activity of ATHB4 (i.e., provided by ATHB4$_{N210A}$). Our results do not allow us to ascertain whether *HAT2* also belongs to this group, at least when growing in different light conditions.

ATHB2 and *HAT2* promoters, but not *SAUR15*, have several putative ATHB4 binding sites (Figure 6A) (Brandt *et al.*, 2012). To investigate whether ATHB4 regulates *ATHB2* and *HAT2* expression by physically interacting with their promoters, we performed ChIP. Our initial attempts using 35S:ATHB4-GFP seedlings failed, likely because the transgenic protein was virtually undetectable by immunoblot analysis (Figure S8). We next used 35S:0HZC-GFP, in which GFP-fused protein levels were easily detectable (Figure S8) and 35S:GFP seedlings as a control (Figure 6B). Three fragments of the *ATHB2* and the *HAT2* promoters (A1 to A3, and H1 to H3, all around putative ATHB4 binding sites) were over-represented in the immunoprecipitated chromatin from 35S:0HZC-GFP seedlings,

in clear contrast with fragments in the CDS of *ATHB2* (A4) and the *UBQ10* (U1) in the same samples, and all these fragments in the immunoprecipitated chromatin from 35S:GFP seedlings (Figure 6). These results indicate that the DNA binding domain of ATHB4 can physically interact with *ATHB2* and *HAT2* promoters *in vivo*. These findings, together with the rapid repression of *ATHB2* and *HAT2* expression upon ATHB4 induction (Figures 3-5) support that these two genes are direct targets of ATHB4 DNA-binding activity.

The DNA-binding activity of ATHB4 is required for regulating leaf polarity in adult plants

To address whether other ATHB4-regulated responses did require its DNA-binding activity, we focused on leaf polarity. The role of ATHB4 in regulating this trait was first visualized by the abaxialization of leaf development in mutant plants deficient in both *ATHB4* and its paralog *HAT3* (Bou-Torrent *et al.*, 2012). Consistently, constitutive overexpression of *ATHB4* (35S:ATHB4-GFP) and DEX-treated 35S:ATHB4-GR plants resulted in upward-curling of leaf blades (Figure S9), a phenotype caused by the relative over-proliferation of abaxial-derived tissues compared to adaxial tissues in leaves (Wenkel *et al.*, 2007; Bou-Torrent *et al.*, 2012). We next analyzed whether some truncated ATHB4 derivatives are functional in controlling leaf curling. Only DEX-induced 35S:NHZ0-GR plants showed upward-curling of leaf blades, like 35S:ATHB4-GR plants. By contrast, DEX-treated 35S:0HZC-GR, 35S:NH00-GR and 35S:ATHB4$_{N210A}$-GR plants, as Col-0, showed no obvious biological activity. The similar expression levels of these transgenes in seedlings and leaves for the lines analyzed (Figures S6, S7E-F, 7A-D) supports that truncated NH00 and mutated ATHB4$_{N210A}$ forms truly have no wild-type activity on leaf polarity. The discrepancies between the activity of these two non-DNA-binding ATHB4 derivatives in the regulation of the shade-induced hypocotyl elongation and the modulation of leaf polarity (Figures 2, 4, 7A-D) suggested that the mechanism of action involved is different: whereas the DNA-binding activity of ATHB4 is required for the regulation of leaf polarity in adult

plants, it is unnecessary (i.e., dispensable) for the control of seedling responses to simulated shade.

The N-terminal region of ATHB4 has a protein-protein interaction domain that is needed for the biological activity

These observations also indicate that the N-terminal region of ATHB4 is important for the control of gene repression in both the SAS seedling responses and leaf polarity. As a first step to understand the molecular mechanism behind the functional regulatory duality of ATHB4, we performed a Y2H screening using full-length ATHB4 as bait. From a total of 63 genes identified, we found HAT2, HAT3, HAT9 and HAT22, encoding HD-Zip II proteins, and TOPLESS (TPL) and TPL-RELATED 4 (TPR4), encoding related transcriptional corepressors (Table S4). The selected interaction domains (SIDs) of the HD-Zip proteins contained all or part of the Zip domain, required for dimerization between family members (Ariel *et al.*, 2007; Brandt *et al.*, 2014). The SIDs of TPL and TPR4 corresponded to the N-terminal region that contains a LisH dimerization domain, proposed to interact with different proteins containing an EAR motif (Brandt *et al.*, 2014). The N-terminal region of ATHB4 (N000) contains two EAR motifs (LxLxL type), one of which (residues 8-12) is conserved among members of the HD-Zip II subfamily (Kagale *et al.*, 2010; Brandt *et al.*, 2014). In Y2H assays, the N000 fragment of ATHB4 could interact with the LisH-containing N-terminal part of TPL (residues 1-242) (Figure 8A). Bimolecular Fluorescence Complementation (BiFC) experiments in agroinfiltrated leaves of *Nicotiana benthamiana* confirmed that full-length ATHB4 binds full-length TPL in the nucleus (Figure 8B). Together, these results suggested that the N-terminal region of ATHB4 can physically interact with TPL *in vivo* likely via the EAR motifs. Although the biological relevance of this interaction is unknown, our results show that the N-terminal part of ATHB4 is involved in interacting with other proteins.

To establish whether EAR motifs within the N-terminal region of ATHB4 were important for its functionality, a truncated form without the first 52 amino acids ($ATHB4_{\Delta N52}$), lacking both EAR domains, was fused to the *GR* gene and

overexpressed in plants (35:ATHB4$_{\Delta N52}$-GR) (Figure 4A). The resulting seedlings displayed a more attenuated DEX-dependent inhibition of hypocotyl elongation in response to W+FR than 35S:ATHB4-GR seedlings, although levels of transgene expression were similar in both cases (Figures 4D, S7F). At the molecular level, the expression of *HAT2* and *SAUR15* genes was unaffected in DEX-treated 35S:ATHB4$_{\Delta N52}$-GR seedlings (+DEX), whereas that of *ATHB2* was up-regulated in 35S:ATHB4$_{\Delta N52}$-GR seedlings, compared to those mock-treated (-DEX) (Figure 4F). These results are consistent with those obtained with the truncated derivatives 00ZC and 0HZC missing the whole Nt-region (Figures 2-3) and confirm that the EAR-containing N-terminal region of ATHB4 has an important role for the modulation of the shade-induced hypocotyl elongation and the repression of gene expression of *HAT2* and, to a lesser extent, *SAUR15*. By contrast, the expression of *ATHB2* can be activated by DNA-binding derivatives of ATHB4 that lack the EAR motifs. When we analyzed the activity of ATHB4$_{\Delta N52}$ in leaf polarity, DEX-treated plants showed no obvious upward curling activity, as it was observed for the 0HZC. The transgene is expressed in leaves to even higher levels than *ATHB4-GR* confirming that mutated ATHB4$_{\Delta N52}$ form has no wild-type activity on leaf polarity (Figure 7E-F).

DISCUSSION

In Arabidopsis seedlings, perception of plant proximity by phytochromes alters a pre-established transcriptional network organized in functional modules that collectively boost elongation growth. Genetics has helped to identify several of the constituents of the functional modules with both positive and negative activities in promoting hypocotyl elongation. Overall, components of the functional modules have the ability to modulate gene expression by at least two major mechanisms: binding to DNA regulatory sequences (i.e., as TFs), or binding to other transcriptional regulators and altering their transcriptional activity (i.e., as transcriptional co-factors) (Wray *et al.*, 2003). A well-known group of SAS components are heterodimers-forming bHLH proteins, in which the positively acting

SAS components are TFs (e.g., PIFs, BEEs, BIMs) and the negative components are transcriptional co-factors (e.g., HFR1, PAR1) (Galstyan *et al.*, 2011; Hornitschek *et al.*, 2012; Cifuentes-Esquivel *et al.*, 2013).

In this manuscript we address the molecular mechanism of action of ATHB4, a member of the HD-Zip II subfamily with a complex role in the SAS hypocotyl elongation. Previous information about other HD-Zip II members suggested a positive role on SAS regulation for ATHB2, HAT1 and HAT2; this conclusion was based mostly on constitutive overexpression phenotypes performed only under high R:FR light (Steindler *et al.*, 1999; Sawa *et al.*, 2002; Ciarbelli *et al.*, 2008). Our analyses using various overexpressing and inducible lines showed that the increased activity of these factors does not promote hypocotyl growth under simulated shade but either had no effect (35S:ATHB2, 35S:HAT2) or even inhibited it (35S:ATHB4-GFP, 35S:HAT1, 35S:ATHB4-GR, 35S:HAT2-GR) (Figure S1). On the other hand, the promotion of hypocotyl elongation under W displayed only by the constitutive lines (Figure S1) might reflect the increased activity of these HD-Zip II proteins in the mother plants and/or embryo development, a kind of preconditioning effect that is absent in the inducible GR-fusion lines, in which DEX is applied from the moment of germination (once the embryo is already formed). The embryo defects observed in the *athb4 hat3* double mutant (Bou-Torrent *et al.*, 2012) support this possibility. Despite the differences observed under W, our results indicate that these factors do not act as SAS positive regulators. In addition, these observations suggested that HD-Zip II members have a similar molecular mechanism of action. Therefore, our analyses place ATHB4 as a paradigm to molecularly understand HD-Zip II members with a similar role in SAS regulation.

Transcriptional regulation by TFs is one of the most investigated mechanisms, as it is generally accepted to be the primary level of regulation (Wray *et al.*, 2003). The emergence of very powerful techniques, such as ChIP combined with next generation sequencing approaches (e.g., ChIP-Seq) or PBMs of recombinant TF proteins combined with bioinformatics analyses, has allowed the experimental characterization of DNA binding motifs and putative target genes bound and regulated by a specific TF. These analyses contribute to unravel the

biological role of the TF through the functional analysis of its targets. By employing PBMs, we could establish that the DNA-binding specificity of ATHB4 does not differ greatly from that of other HD-Zip II proteins studied. The absence of DNA-binding activity of the mutant ATHB4$_{N210A}$ protein indicates that the HD is required for this function, as expected, and that no other region of ATHB4 (such as the conserved N-terminal region of unknown function) has DNA-binding activity (Figure 4). Transcriptome analyses performed using the inducible 35S:ATHB4-GR line showed that ATHB4 acts fundamentally as a transcriptional repressor, as described for other HD-Zip II members (Steindler *et al.*, 1999; Ohgishi *et al.*, 2001; Sawa *et al.*, 2002) and in contrast with HD-Zip III proteins that act as transcriptional activators (Xie *et al.*, 2015). Surprisingly, only a small proportion of the ATHB4 putative target genes are also rapidly shade regulated, which supports other roles for ATHB4 in plant development (e.g., leaf polarity).

Our structure-function analyses led to go further in the current understanding of this type of transcriptional regulators. On one hand, we show that truncated ATHB4 fragments containing only the HD-Zip domains (e.g., 0HZ0 and 0HZC) are not sufficient to confer full activity in the repression of the shade-induced hypocotyl elongation and specific gene expression, and that the missing N-terminal region contains information to interact with other proteins (Figure 8) that is required for the wild-type biological activity of ATHB4. This conserved region of unknown function is very likely functionally necessary for all the members of the HD-Zip II subfamily. On the other hand, ATHB4 derivatives unable to bind DNA (truncated NH00 and ATHB4$_{N210A}$) are fully functional in inhibiting both the shade-induced hypocotyl elongation and up-regulation of *HAT2* and *SAUR15*. Since *SAUR15* is directly regulated by ATHB4 even when it has lost its ability to bind DNA (Table S3, Figure 5), these results suggest the unexpected possibility that a part of the ATHB4 mechanism of action involves modulating gene expression without direct binding to regulatory regions of the DNA, i.e., ATHB4 acts also as a transcription cofactor (Figure 9). This possibility is supported by our transcriptome analyses that show that the majority of the ATHB4 putative direct target genes (69 out of a total of 104 genes, i.e., ~66 %) lack 9-mer DNA binding motifs for ATHB4

in their promoter regions, among which *SAUR15* can be found (Table S3). The co-factor activity requires that either ATHB4 (i) accesses promoters via proteins that can themselves bind DNA, or (ii) impedes other transcription factors to bind to their *cis*-regulatory targets. In either case, this activity is likely sustained in the protein-protein abilities of the N-terminal region (e.g., via the EAR domain), which is conserved between the members of this subfamily.

After these analyses, one might wonder why ATHB4 has a DNA-binding activity that is dispensable for its function *in vivo*. One possibility is that other ATHB4-dependent functions do require its DNA-binding activity. Indeed, our analyses indicate that ATHB4 acts as a bona fide TF in controlling leaf polarity, an activity shared with other HD-Zip II members (Bou-Torrent *et al.*, 2012; Turchi *et al.*, 2013). Leaf flattening is also promoted by end-of-day-FR, a treatment that mimics plant proximity (Kozuka *et al.*, 2013). Recently it has been suggested that ATHB4, together with its paralog HAT3, might be part of the mechanisms regulating this SAS response in adult leaves (Roig-Villanova & Martinez-Garcia, 2016). As in the modulation of the SAS hypocotyl elongation response, the control of leaf polarity requires the EAR-containing first 52 residues of ATHB4; but in contrast, the DNA-binding activity is not dispensable (Figure 7).

It seems therefore that ATHB4 would have two activities, one DNA-binding dependent and another DNA-binding independent (Figure 9). Although in physiological conditions, both activities cannot be uncoupled, it is reasonable to postulate that both activities are not working equally. Genetics suggests that the leaf polarity phenotype (ATHB4 DNA-binding dependent), requires very low levels of *ATHB4* expression (e.g., even single *athb4* and *hat3* loss-of-function mutants display a wild-type phenotype) (Sorin *et al.*, 2009). In this framework, the DNA-binding dependent activity of ATHB4 might act as a molecular switch to trigger the normal cotyledon and leaf development: when there is no ATHB4 (and HAT3) activity, the switch is off, seedling cotyledons (the site of shade perception) are defective, and the shade-induced hypocotyl elongation is impaired. And when cotyledons are developing properly, the additional transcriptional cofactor activity has a role. This activity would most likely take place when cellular levels of ATHB4

are relatively higher. Indeed, *ATHB4* expression (and that of many other *PAR* genes) is strongly promoted by shade exposure in a R:FR-dependent manner: the lower R:FR, the higher *ATHB4* expression (Roig-Villanova *et al.*, 2006). The shade-induced hypocotyl length is also strongly dependent on the R:FR, and when the R:FR is very low (precisely when *ATHB4* expression is highest), hypocotyl elongation is inhibited by the antagonistic effect of phyA (Martinez-Garcia *et al.*, 2014). These very low R:FR conditions mimic natural situation of deep shade, when canopy closure occurs (Yanovsky *et al.*, 1995). Therefore, the non-DNA-binding activity of ATHB4 can contribute to the optimal hypocotyl elongation response under conditions of deep shade.

Is this dual molecular activity of ATHB4 a unique case among TFs? There are few reports indicating that this is not the case. Functional analysis of three closely related bHLH members, SPEECHLESS (SPCH), MUTE, and FAMA, which have distinct functions regulating sequential steps of stomata development, provided surprising evidence that, despite deep sequence conservation in their DNA-binding domains, both SPCH and MUTE do not require DNA-binding activity for their *in vivo* activities in regulating this response (Davies & Bergmann, 2014). A mutated PIF3 form unable to bind DNA was shown to fully complement the *pif3* mutation in terms of the hypocotyl response to monochromatic R, whereas the mutated form unable to bind to the phyB photoreceptor was inactive in complementing this trait (Al-Sady *et al.*, 2008). These results indicated that, like in ATHB4, PIF3 DNA-binding was unnecessary to modulate hypocotyl elongation in response to specific light conditions (monochromatic R). Like ATHB4, PIF3 also contains an additional region involved in protein-protein interactions (i.e., the APB domain involved in interacting with the phyB photoreceptors). Our results suggest that all these proteins might be involved in regulating other responses as TFs: in the case of PIF3, it might be also involved in the control of carotenoid biosynthesis by directly regulating *PSY* gene expression (Toledo-Ortiz *et al.*, 2010; Bou-Torrent *et al.*, 2015).

A level of genome plasticity resides in the ability of a single gene to produce different protein isoforms via alternative splicing regulated by external stimuli (Pose

et al., 2013; Nicolas *et al.*, 2015). The functional duality of these HD-Zip II regulators acting either as a transcriptional factor or cofactor in the regulation of different developmental responses reveals an additional level of genome plasticity, in this case in different developmental processes. What are the determinants that drive the use of the possible molecular mechanisms is currently unknown, although we envisage that cellular levels and the spatial and temporal expression of additional partners (via the N-terminal region) might be important.

In summary, we have functionally analyzed the mechanism of action of ATHB4, a specific factor that regulates the SAS and leaf polarity. Our results indicated that the DNA-binding activity of ATHB4 is not required for the regulation of the SAS seedling responses (Figure 9). These findings suggest that, when working with a protein containing canonical and functional DNA-binding domains, it cannot be assumed that the studied protein acts essentially as a TF, i.e., that the basic mechanism of control of target gene expression action involves only binding to specific *cis*-acting regulatory sequences. Therefore, our results expand our current view and understanding of the function of TFs as mere DNA-binding proteins with transcriptional activity.

ACKNOWLEDGEMENTS

We are grateful to the greenhouse service for plant care; to Montse Amenòs for help and support with confocal microscopy; to Alejandro Ferrando (IBMCP, Valencia, Spain) for BiFC vectors; to Stephan Wenkel (Copenhagen Plant Science Centre, Denmark) for pENTR-TPL; to Masahiro Yano (National Institute of Agrobiological Research, Ibarahi, Japan) for pPZP-Hd1(SG) vector; to Ida Ruberti (Institute of Molecular Biology and Pathology, CNR, Rome, Italy) for 35S:ATHB2 and 35S:HAT2 seeds; and Irma Roig-Villanova and Manuel Rodríguez-Concepción (CRAG) for comments on the manuscript. MG and MJM-C received predoctoral FPI fellowships from the Spanish Ministry of Economy and Competivity (MINECO). SP received a predoctoral fellowship from Catalan Agència de Gestió d'Ajuts Universitaris i de Recerca (AGAUR, FI-DGR 2015). MS-M received a predoctoral fellowship from the CSIC (JAEpre program). CS financial support came from the

AGAUR (C-RED Program). Our research is supported by grants from the MINECO-FEDER (BIO2011-23489, BIO2014-59895-P) and AGAUR (2014-SGR447 and Xarba) to JFM-G. We also acknowledge the support of the MINECO for the "Centro de Excelencia Severo Ochoa 2016-2019" award SEV-2015-0533 and the Generalitat de Catalunya by the CERCA Program.

AUTHOR CONTRIBUTIONS

MG, MJM-C, SP, MS-M, CS, MG, JMF-Z, RS and JFM-G conducted the experiments, analyzed data and designed the experiments; MG, MJM-C, SP, JMF-Z and JFM-G wrote the paper.

REFERENCES

Al-Sady B, Kikis EA, Monte E, Quail PH. 2008. Mechanistic duality of transcription factor function in phytochrome signaling. *Proceedings of the National Academy of Sciences, USA* **105**: 2232-2237.

Ariel FD, Manavella PA, Dezar CA, Chan RL. 2007. The true story of the HD-Zip family. *Trends in Plant Science* **12**: 419-426.

Bou-Torrent J, Salla-Martret M, Brandt R, Musielak T, Palauqui JC, Martinez-Garcia JF, Wenkel S. 2012. ATHB4 and HAT3, two class II HD-ZIP transcription factors, control leaf development in *Arabidopsis*. *Plant Signaling & Behavior* **7**: 1382-1387.

Bou-Torrent J, Toledo-Ortiz G, Ortiz-Alcaide M, Cifuentes-Esquivel N, Halliday KJ, Martinez-Garcia JF, Rodriguez-Concepcion M. 2015. Regulation of Carotenoid Biosynthesis by Shade Relies on Specific Subsets of Antagonistic Transcription Factors and Cofactors. *Plant Physiology* **169**: 1584-1594.

Brandt R, Cabedo M, Xie Y, Wenkel S. 2014. Homeodomain leucine-zipper proteins and their role in synchronizing growth and development with the environment. *Journal of Integrative Plant Biology* **56**: 518-526.

Brandt R, Salla-Martret M, Bou-Torrent J, Musielak T, Stahl M, Lanz C, Ott F, Schmid M, Greb T, Schwarz M, et al. 2012. Genome-wide binding-site analysis of REVOLUTA reveals a link between leaf patterning and light-mediated growth responses. *Plant Journal* **72**: 31-42.

Casal JJ. 2013. Photoreceptor signaling networks in plant responses to shade. *Annual Review of Plant Biology* **64**: 403-427.

Ciarbelli AR, Ciolfi A, Salvucci S, Ruzza V, Possenti M, Carabelli M, Fruscalzo A, Sessa G, Morelli G, Ruberti I. 2008. The *Arabidopsis* homeodomain-leucine zipper II gene family: diversity and redundancy. *Plant Molecular Biology* **68**: 465-478.

Cifuentes-Esquivel N, Bou-Torrent J, Galstyan A, Gallemi M, Sessa G, Salla Martret M, Roig-Villanova I, Ruberti I, Martinez-Garcia JF. 2013. The

bHLH proteins BEE and BIM positively modulate the shade avoidance syndrome in *Arabidopsis* seedlings. *Plant Journal* **75**: 989-1002.

Crocco CD, Holm M, Yanovsky MJ, Botto JF. 2010. AtBBX21 and COP1 genetically interact in the regulation of shade avoidance. *Plant Journal* **64**: 551-562.

Crocco CD, Locascio A, Escudero CM, Alabadi D, Blazquez MA, Botto JF. 2015. The transcriptional regulator BBX24 impairs DELLA activity to promote shade avoidance in *Arabidopsis thaliana*. *Nature Communications* **6**: 6202.

Davies KA, Bergmann DC. 2014. Functional specialization of stomatal bHLHs through modification of DNA-binding and phosphoregulation potential. *Proceedings of the National Academy of Sciences, USA* **111**: 15585-15590.

Faigon-Soverna A, Harmon FG, Storani L, Karayekov E, Staneloni RJ, Gassmann W, Mas P, Casal JJ, Kay SA, Yanovsky MJ. 2006. A constitutive shade-avoidance mutant implicates TIR-NBS-LRR proteins in *Arabidopsis* photomorphogenic development. *Plant Cell* **18**: 2919-2928.

Franco-Zorrilla JM, Lopez-Vidriero I, Carrasco JL, Godoy M, Vera P, Solano R. 2014. DNA-binding specificities of plant transcription factors and their potential to define target genes. *Proceedings of the National Academy of Sciences, USA* **111**: 2367-2372.

Galstyan A, Cifuentes-Esquivel N, Bou-Torrent J, Martinez-Garcia JF. 2011. The shade avoidance syndrome in *Arabidopsis*: a fundamental role for atypical basic helix-loop-helix proteins as transcriptional cofactors. *Plant Journal* **66**: 258-267.

Gallemi M, Galstyan A, Paulisic S, Then C, Ferrandez-Ayela A, Lorenzo-Orts L, Roig-Villanova I, Wang X, Micol JL, Ponce MR, et al. 2016. DRACULA2 is a dynamic nucleoporin with a role in regulating the shade avoidance syndrome in *Arabidopsis*. *Development* **143**: 1623-1631.

Godoy M, Franco-Zorrilla JM, Perez-Perez J, Oliveros JC, Lorenzo O, Solano R. 2011. Improved protein-binding microarrays for the identification of DNA-binding specificities of transcription factors. *Plant Journal* **66**: 700-711.

Hornitschek P, Kohnen MV, Lorrain S, Rougemont J, Ljung K, Lopez-Vidriero I, Franco-Zorrilla JM, Solano R, Trevisan M, Pradervand S, et al. 2012. Phytochrome interacting factors 4 and 5 control seedling growth in changing light conditions by directly controlling auxin signaling. *Plant Journal* **71**: 699-711.

Kagale S, Links MG, Rozwadowski K. 2010. Genome-wide analysis of ethylene-responsive element binding factor-associated amphiphilic repression motif-containing transcriptional regulators in *Arabidopsis*. *Plant Physiology* **152**: 1109-1134.

Kozuka T, Suetsugu N, Wada M, Nagatani A. 2013. Antagonistic regulation of leaf flattening by phytochrome B and phototropin in *Arabidopsis thaliana*. *Plant & Cell Physiology* **54**: 69-79.

Leivar P, Quail PH. 2011. PIFs: pivotal components in a cellular signaling hub. *Trends in Plant Science* **16**: 19-28.

Li L, Ljung K, Breton G, Schmitz RJ, Pruneda-Paz J, Cowing-Zitron C, Cole BJ, Ivans LJ, Pedmale UV, Jung HS, et al. 2012. Linking photoreceptor

excitation to changes in plant architecture. *Genes & Development* **26**: 785-790.

Lorrain S, Allen T, Duek PD, Whitelam GC, Fankhauser C. 2008. Phytochrome-mediated inhibition of shade avoidance involves degradation of growth-promoting bHLH transcription factors. *Plant Journal* **53**: 312-323.

Martinez-Garcia JF, Galstyan A, Salla-Martret M, Cifuentes-Esquivel N, Gallemí M, Bou-Torrent J. 2010. Regulatory components of shade avoidance syndrome. *Advances in Botanical Research* **53**: 65-116.

Martinez-Garcia JF, Gallemi M, Molina-Contreras MJ, Llorente B, Bevilaqua MR, Quail PH. 2014. The shade avoidance syndrome in *Arabidopsis*: the antagonistic role of phytochrome a and B differentiates vegetation proximity and canopy shade. *PLoS One* **9**: e109275.

Nicolas M, Rodriguez-Buey ML, Franco-Zorrilla JM, Cubas P. 2015. A Recently Evolved Alternative Splice Site in the *BRANCHED1a* Gene Controls Potato Plant Architecture. *Current Biology* **25**: 1799-1809.

Ohgishi M, Oka A, Morelli G, Ruberti I, Aoyama T. 2001. Negative autoregulation of the *Arabidopsis* homeobox gene *ATHB-2*. *Plant Journal* **25**: 389-398.

Pose D, Verhage L, Ott F, Yant L, Mathieu J, Angenent GC, Immink RG, Schmid M. 2013. Temperature-dependent regulation of flowering by antagonistic FLM variants. *Nature* **503**: 414-417.

Reymond MC, Brunoud G, Chauvet A, Martinez-Garcia JF, Martin-Magniette ML, Moneger F, Scutt CP. 2012. A light-regulated genetic module was recruited to carpel development in *Arabidopsis* following a structural change to SPATULA. *Plant Cell* **24**: 2812-2825.

Roig-Villanova I, Bou-Torrent J, Galstyan A, Carretero-Paulet L, Portoles S, Rodriguez-Concepcion M, Martinez-Garcia JF. 2007. Interaction of shade avoidance and auxin responses: a role for two novel atypical bHLH proteins. *EMBO Journal* **26**: 4756-4767.

Roig-Villanova I, Bou J, Sorin C, Devlin PF, Martinez-Garcia JF. 2006. Identification of primary target genes of phytochrome signaling. Early transcriptional control during shade avoidance responses in *Arabidopsis*. *Plant Physiology* **141**: 85-96.

Roig-Villanova I, Martinez-Garcia JF. 2016. Plant Responses to Vegetation Proximity: A Whole Life Avoiding Shade. *Frontiers in Plant Science* **7**: 236.

Sawa S, Ohgishi M, Goda H, Higuchi K, Shimada Y, Yoshida S, Koshiba T. 2002. The *HAT2* gene, a member of the HD-Zip gene family, isolated as an auxin inducible gene by DNA microarray screening, affects auxin response in *Arabidopsis*. *Plant Journal* **32**: 1011-1022.

Sessa G, Carabelli M, Sassi M, Ciolfi A, Possenti M, Mittempergher F, Becker J, Morelli G, Ruberti I. 2005. A dynamic balance between gene activation and repression regulates the shade avoidance response in *Arabidopsis*. *Genes & Development* **19**: 2811-2815.

Sessa G, Morelli G, Ruberti I. 1997. DNA-binding specificity of the homeodomain-leucine zipper domain. *Journal of Molecular Biology* **274**: 303-309.

Sorin C, Salla-Martret M, Bou-Torrent J, Roig-Villanova I, Martinez-Garcia JF. 2009. ATHB4, a regulator of shade avoidance, modulates hormone response in *Arabidopsis* seedlings. *Plant Journal* **59**: 266-277.

Steindler C, Matteucci A, Sessa G, Weimar T, Ohgishi M, Aoyama T, Morelli G, Ruberti I. 1999. Shade avoidance responses are mediated by the ATHB-2 HD-zip protein, a negative regulator of gene expression. *Development* **126**: 4235-4245.

Toledo-Ortiz G, Huq E, Rodriguez-Concepcion M. 2010. Direct regulation of phytoene synthase gene expression and carotenoid biosynthesis by phytochrome-interacting factors. *Proceedings of the National Academy of Sciences, USA* **107**: 11626-11631.

Turchi L, Baima S, Morelli G, Ruberti I. 2015. Interplay of HD-Zip II and III transcription factors in auxin-regulated plant development. *Journal of Experimental Botany* **66**: 5043-5053.

Turchi L, Carabelli M, Ruzza V, Possenti M, Sassi M, Penalosa A, Sessa G, Salvi S, Forte V, Morelli G, et al. 2013. Arabidopsis HD-Zip II transcription factors control apical embryo development and meristem function. *Development* **140**: 2118-2129.

Wenkel S, Emery J, Hou BH, Evans MM, Barton MK. 2007. A feedback regulatory module formed by LITTLE ZIPPER and HD-ZIPIII genes. *Plant Cell* **19**: 3379-3390.

Wray GA, Hahn MW, Abouheif E, Balhoff JP, Pizer M, Rockman MV, Romano LA. 2003. The evolution of transcriptional regulation in eukaryotes. *Mol Biol Evol* **20**: 1377-1419.

Xie Y, Straub D, Eguen T, Brandt R, Stahl M, Martinez-Garcia JF, Wenkel S. 2015. Meta-Analysis of Arabidopsis KANADI1 Direct Target Genes Identifies a Basic Growth-Promoting Module Acting Upstream of Hormonal Signaling Pathways. *Plant Physiology* **169**: 1240-1253.

Yanovsky MJ, Casal JJ, Whitelam GC. 1995. Phytochrome A, phytochrome B and HY4 are invovled in hypocotyl growth responses to natural radiation in *Arabidopsis*: Weak de-etiolation of the phyA mutant under dense canopies. *Plant, Cell & Environment* **18**: 788-794.

SUPPORTING INFORMATION

Additional supporting information may be found in the online version of this article.

Fig. S1. Phenotypic analyses of seedlings over-expressing *ATHB2*, *HAT2*, *HAT1*, *HAT2-GR*, *ATHB4-GFP* and *ATHB4-GR*.

Fig. S2. Evaluation of biological relevance of DNA-motifs from co-regulation information.

Fig. S3. Analysis of the homodimerization activity of the HD-Zip region of ATHB4.

Fig. S4. Subcellular localization of ATHB4 and its derivatives.

FIGURE LEGENDS

Figure 1. ATHB4 acts as a DNA-binding factor that represses gene expression. **(A)** Microarrays were performed with RNA extracted from 7-day-old 35S:ATHB4-GR transgenic *Arabidopsis thaliana* seedlings grown under continuous white light (W) harvested (white circle) 4 h after treatment with or without dexamethasone DEX in presence or absence of the protein synthesis inhibitor cycloheximide (CHX). **(B)** Venn diagrams illustrating the overlap of DEX-regulated genes in

seedlings treated without (left) and with (right) CHX. The total number of genes in each group is indicated in parentheses. The group of overlapping genes is considered to be directly regulated by ATHB4. FC, fold change. **(C)** DNA-binding specificity of ATHB4. Position weight matrix (PWM) representation of the top scoring 7-mer and 9-mer consensus sequences preferentially bound by ATHB4. **(D)** Box-plot of enrichment scores (E-scores) of the 7-mer box consensus including three site-directed mutant variants of the top scoring shown in **C**. Boxes represent quartiles 25–75% and the black line represents the median of the distribution (quartile 50%). Bars indicate quartiles 1–25% (above) and 75–100% (below). Dots denote outliers of the distribution.

Figure 2. Hypocotyl elongation of *Arabidopsis thaliana* seedlings overexpressing truncated derivatives of ATHB4. **(A)** Cartoon detailing the truncated ATHB4 derivatives overexpressed in plants. **(B)** Summary of growth conditions: seeds were sown in media supplemented without (-DEX) or with dexamethasone (+DEX). Seedlings were germinated and grown for 2 days in continuous white light (W) and then transferred to W enriched in far-red light (W+FR) for 5 more days. **(C)** Ratio of hypocotyl length of seedlings grown in +DEX and –DEX media as indicator of ATHB4 biological activity. Bars represent the mean ± SE. In each graph, white bars correspond to the wild-type (Col-0), black bars to the 35S:ATHB4-GR line and light grey bars to the ATHB4 derivative line. Asterisks indicate significant differences (*P<0.05, **P<0.01) relative to the wild-type control.

Figure 3. Molecular responses of *Arabidopsis thaliana* seedlings overexpressing truncated versions of ATHB4 to simulated shade. **(A)** Seedlings were germinated and grown for 7 days in media supplemented (+DEX) or not (–DEX) with dexamethasone (DEX) under continuous white light (W). Samples were harvested after 1h of W enriched in far-red light (W+FR) treatment (white circle). Each RNA sample was extracted from a pool of homozygous seedlings. **(B-F)** Transcript abundances of *HAT2*, *SAUR15* and *ATHB2* genes, normalized to *UBQ10*, are shown in the indicated transgenic lines. Gene expression is presented relative to

the levels of the analyzed gene in wild-type (Col-0) seedlings without DEX treatment. Values are means ± SE of three independent RT-qPCR biological replicates. White and blue columns correspond to –DEX and +DEX samples, respectively. Asterisks indicate significant differences in transcript levels (Student *t* test, *P<0.05, **P<0.01) between –DEX and +DEX treatments.

Figure 4. Seedling responses of transgenic lines overexpressing mutated ATHB4$_{N210A}$ and ATHB4$_{\Delta N52}$. **(A)** Cartoon detailing the mutated *ATHB4$_{N210A}$* and ATHB4$_{\Delta N52}$ derivatives overexpressed in *Arabidopsis thaliana* plants. Black circle on top of a vertical line represents the location of the introduced point mutation. **(B)** Comparison of the box-plot enrichment scores (E-scores) with the 7- and 8-mer box consensus and the top scoring site-directed mutant variants for ATHB4 and ATHB4$_{N210A}$. Boxes represent quartiles 25–75% and the black line represents the median of the distribution (quartile 50%). Bars indicate quartiles 1–25% (above) and 75–100% (below). Dots denote outliers of the distribution. **(C, D)** Ratio of hypocotyl length of seedlings grown in +DEX and –DEX media for the 35S:ATHB4$_{N210A}$-GR **(C)** and 35S: ATHB4$_{\Delta N52}$-GR **(D)** lines. Seeds were sown in media supplemented without (-DEX) or with dexamethasone (+DEX). Seedlings were germinated and grown for 2 days in continuous white light (W) and then transferred to W enriched in far-red light (W+FR) for 5 more days. Bars represent the mean ± SE. White, black and light grey bars correspond to the wild-type (Col-0), 35S:ATHB4-GR and derivative lines, respectively. Symbols indicate significant differences (*P<0.05, **P<0.01) relative to the control. **(E, F)** Transcript abundances of *HAT2, SAUR15* and *ATHB2* genes, normalized to *UBQ10*, in seedlings of Col-0, 35S:ATHB4-GR, 35S:ATHB4$_{N210A}$-GR **(E)** and ATHB4$_{\Delta N52}$-GR **(F)**. Seedlings were germinated and grown for 7 days in media supplemented (+DEX) or not (–DEX) with dexamethasone (DEX) under W. Samples were harvested after 1h of W+FR treatment. Gene expression is presented relative to levels in Col-0 without DEX treatment. Values are means ± SE of three independent RT-qPCR biological replicates. White and blue columns correspond to –DEX and +DEX samples, respectively. Asterisks indicate significant differences in

transcript levels (Student *t* test, *P<0.05, **P<0.01) between –DEX and +DEX treatments. DEX, dexamethasone.

Figure 5. Identification of direct target genes of non-DNA-binding derivatives of ATHB4. **(A)** *Arabidopsis thaliana* seedlings were germinated and grown for 7 days under white light (W) and then treated during 4 hours with or without dexamethasone (DEX) in the presence or absence of cycloheximide (CHX). Samples were harvested after irradiation with W enriched with far-red light (W+FR) provided during the last hour of the ±DEX/±CHX treatment. Each RNA samples was extracted from a pool of homozygous seedlings. **(B)** Transcript abundances of *HAT2*, *SAUR15* and *ATHB2* genes, normalized to *UBQ10*, in Col-0, 35S:ATHB4-GR, 35S:NH00-GR and $ATHB4_{N210A}$-GR seedlings grown as detailed in **A**. Gene expression is presented relative to levels in Col-0 without DEX and CHX treatments. Values are means ± SE of three independent RT-qPCR biological replicates. White and blue columns correspond to –DEX and +DEX samples, respectively. Asterisks indicate significant differences in transcript levels (Student *t* test, *P<0.05, **P<0.01) between –DEX and +DEX treatments for a given CHX application.

Figure 6. The DNA-binding domain of ATHB4 binds in vivo in Chromatin immunoprecipitation (ChIP) assays to different regions of the *ATHB2* and *HAT2* promoters. **(A)** Schematic representation of the genomic *ATHB2*, *HAT2* and *UBQ10* genes. The position of the 7 mer ATHB4-binding sites is represented using empty blue (AATGATT) and orange (ATTAATT) triangles. Upper and lower triangles indicate whether these sites are located in the sense and antisense DNA strands, respectively. The location of the amplified DNA fragments is represented with a thick black line in the genomic *ATHB2* (A1 to A4), *HAT2* (H1 to H3) and *UBQ10* (U1) genes. **(B)** Cartoon detailing the GFP-tagged *Arabidopsis thaliana* transgenic lines used for the ChIP assay. **(C)** ChIP assays were carried out using a 35S:0HZC-GFP line with antibodies against the GFP (+antiGFP). A 35S:GFP line was used as a control. A second set of samples were processed without antibody

(-antiGFP) and used as negative controls. The average fold enrichment of DNA fragments in the +antiGFP samples compared to the -antiGFP samples in relation to the total chromatin input is shown. Error bars indicate ±SE of three biological triplicates.

Figure 7. Leaf polarity phenotypes of *Arabidopsis thaliana* plants overexpressing derivatives of *ATHB4*. **(A, C, E)** Effect of dexamethasone (DEX) treatment on leaf polarity: adaxial view (ad) in the upper part, abaxial view (ab) on the middle and transverse representation on lower part. Wild-type (Col-0), and overexpressing *ATHB4-GR*, *NHZ0-GR*, *0HCZ-GR*, *NH00-GR* (A), $ATHB4_{N210A}$*-GR* **(C)** and $ATHB4_{\Delta N52}$*-GR* **(E)** plants were grown under short day conditions. On day 21 after germination, plants were treated with 5 µM DEX by adding a drop of 10 µl to the apical meristem. During a total of 10 days, plants were treated almost daily (7 times). On day 30, newly formed leaves were detached from the plant and photographed. Within a section, leaves are shown to the same scale. Scale bar = 1 cm. **(B, D, F)** Transcript abundances of the GR-fused transgenes normalized to *UBQ10* in the indicated transgenic lines. Transcripts were quantified by RT-qPCR with specific *GR* primers and using pools of three leaves from the same experiment as a sample. Gene expression is presented relative to levels in 35S:ATHB4-GR leaves on day 30. Values are means ± SE of three independent RT-qPCR biological replicates. Asterisks indicate significant differences in transcript levels (Student *t* test, *P<0.05, **P<0.01) relative to the 35S:ATHB4-GR line.

Figure 8. The Nt region of ATHB4 (N) has protein-protein interaction activity. **(A)** Experimental design of the specific combinations (#1 to 9) of DNA-binding domain (BD) and activation domain (AD) yeast constructs used in the assay (left side) and dilution spots of the yeast strains (right side). SD-LW and SD-HLW refer to the selective media indicative of transformed cells or interaction between the hybrid proteins, respectively. All transformations were repeated at least twice with identical results. Truncated forms of murine p53 (fused to BD) and SV40 large T-antigen (fused to AD), known to interact, and empty vectors are used as positive

(#1) and negative (#2) controls in this growth assay, respectively. **(B)** Bimolecular fluorescence complementation (BiFC) in *Nicotiana benthamiana* leaves 3 days after agroinfiltration with the indicated YN and YC fusions (for the final YFP reconstitution). Confocal images of fluorescence in epidermal cells (upper side) and overlap with bright-field images (lower side) are shown. Scale bar = 100 μm.

Figure 9. Summary of ATHB4 molecular and physiological activities studied in this work. ATHB4 interacts through the N-terminal (N) region with other proteins. ATHB4 binds to DNA as a dimer through the HD-Zip (HZ) domains. The interaction with proteins through the N region seems to be essential to regulate gene expression, but ATHB4 does not require dimerization or DNA binding for shade related activities in seedlings, acting as a Transcription Cofactor. Both activities (DNA-binding and interaction with other proteins) are required for controlling leaf polarity, suggesting that ATHB4 acts as a Transcription Factor on this trait.

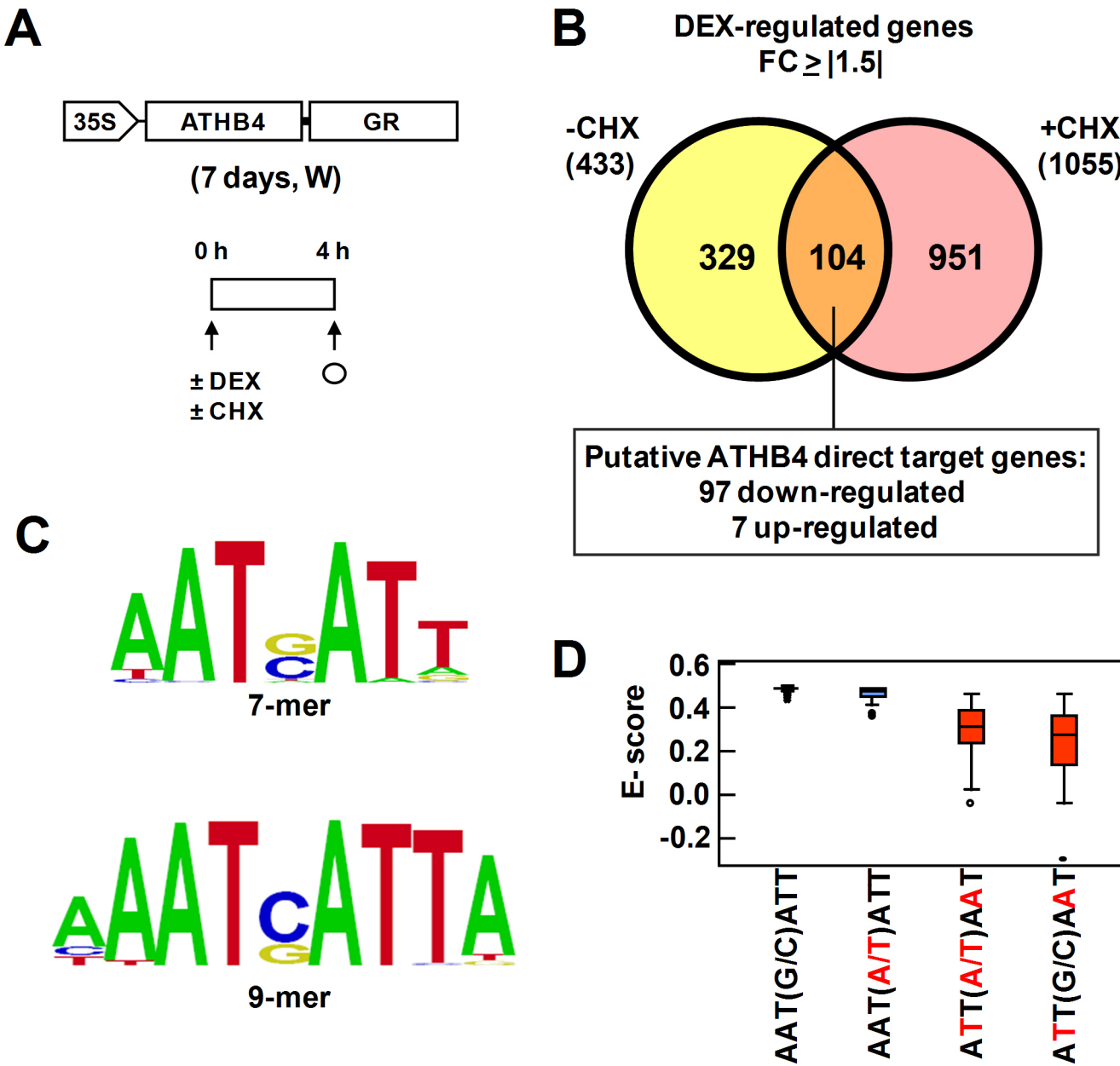
A
35S
ATHB4
GR
(7 days, W)
0 h
4 h
± DEX
± CHX
B
DEX-regulated genes
FC ≥ |1.5|
-CHX
(433)
+CHX
(1055)
329
104
951
Putative ATHB4 direct target genes:
97 down-regulated
7 up-regulated
C
7-mer
9-mer
D
E- score
0.6
0.4
0.2
0.0
-0.2
AAT(G/C)ATT
AAT(A/T)ATT
ATT(A/T)AAT
ATT(G/C)AAT

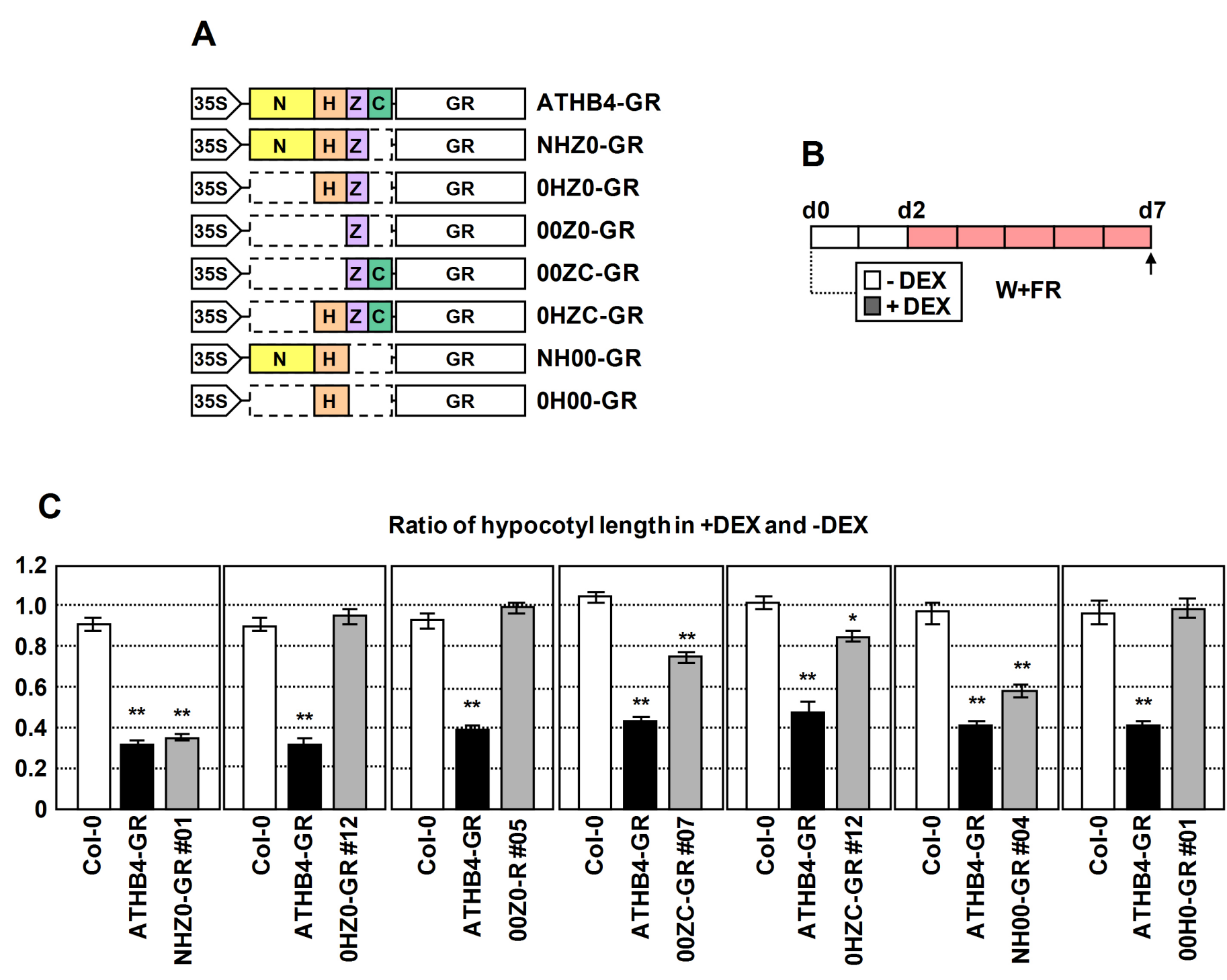
A
35S
N
H
Z
C
GR
ATHB4-GR
NHZ0-GR
0HZ0-GR
00Z0-GR
00ZC-GR
0HZC-GR
NH00-GR
0H00-GR
B
d0
d2
d7
- DEX
+ DEX
W+FR
C
Ratio of hypocotyl length in +DEX and -DEX
1.2
1.0
0.8
0.6
0.4
0.2
0
**
*
Col-0
ATHB4-GR
NHZ0-GR #01
0HZ0-GR #12
00Z0-R #05
00ZC-GR #07
0HZC-GR #12
NH00-GR #04
00H0-GR #01

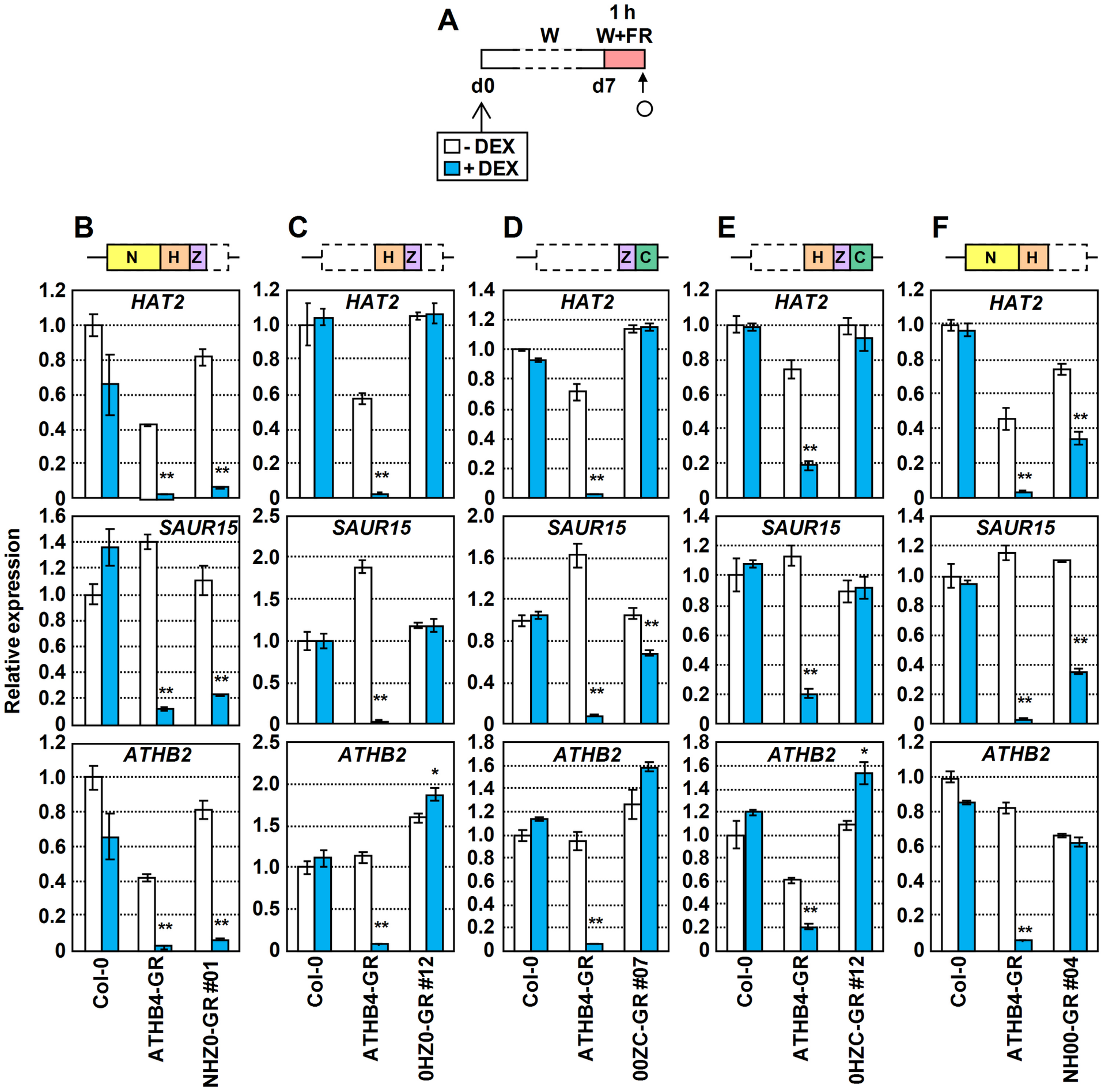
A
1 h
W
W+FR
d0
d7
- DEX
+ DEX
B
C
D
E
F
N
H
Z
C
HAT2
SAUR15
ATHB2
Relative expression
Col-0
ATHB4-GR
NHZ0-GR #01
0HZ0-GR #12
00ZC-GR #07
0HZC-GR #12
NH00-GR #04

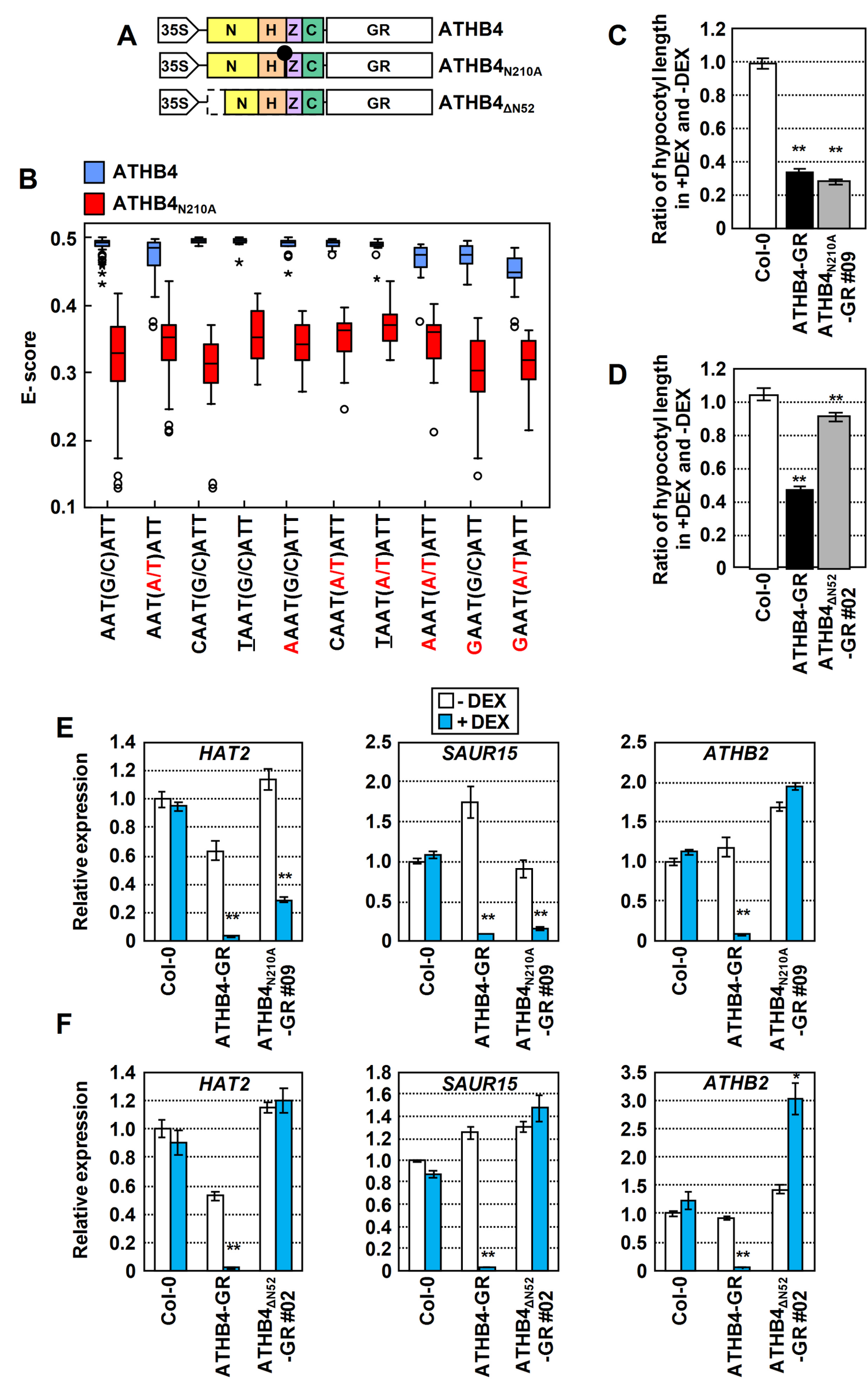
A
35S
N
H
Z
C
GR
ATHB4
ATHB4N210A
ATHB4ΔN52
B
ATHB4
ATHB4N210A
E- score
AAT(G/C)ATT
AAT(A/T)ATT
CAAT(G/C)ATT
TAAT(G/C)ATT
AAAT(G/C)ATT
CAAT(A/T)ATT
TAAT(A/T)ATT
AAAT(A/T)ATT
GAAT(G/C)ATT
GAAT(A/T)ATT
C
Ratio of hypocotyl length in +DEX and -DEX
Col-0
ATHB4-GR
ATHB4N210A -GR #09
D
Ratio of hypocotyl length in +DEX and -DEX
Col-0
ATHB4-GR
ATHB4ΔN52 -GR #02
E
- DEX
+ DEX
Relative expression
HAT2
SAUR15
ATHB2
Col-0
ATHB4-GR
ATHB4N210A -GR #09
F
Relative expression
HAT2
SAUR15
ATHB2
Col-0
ATHB4-GR
ATHB4ΔN52 -GR #02

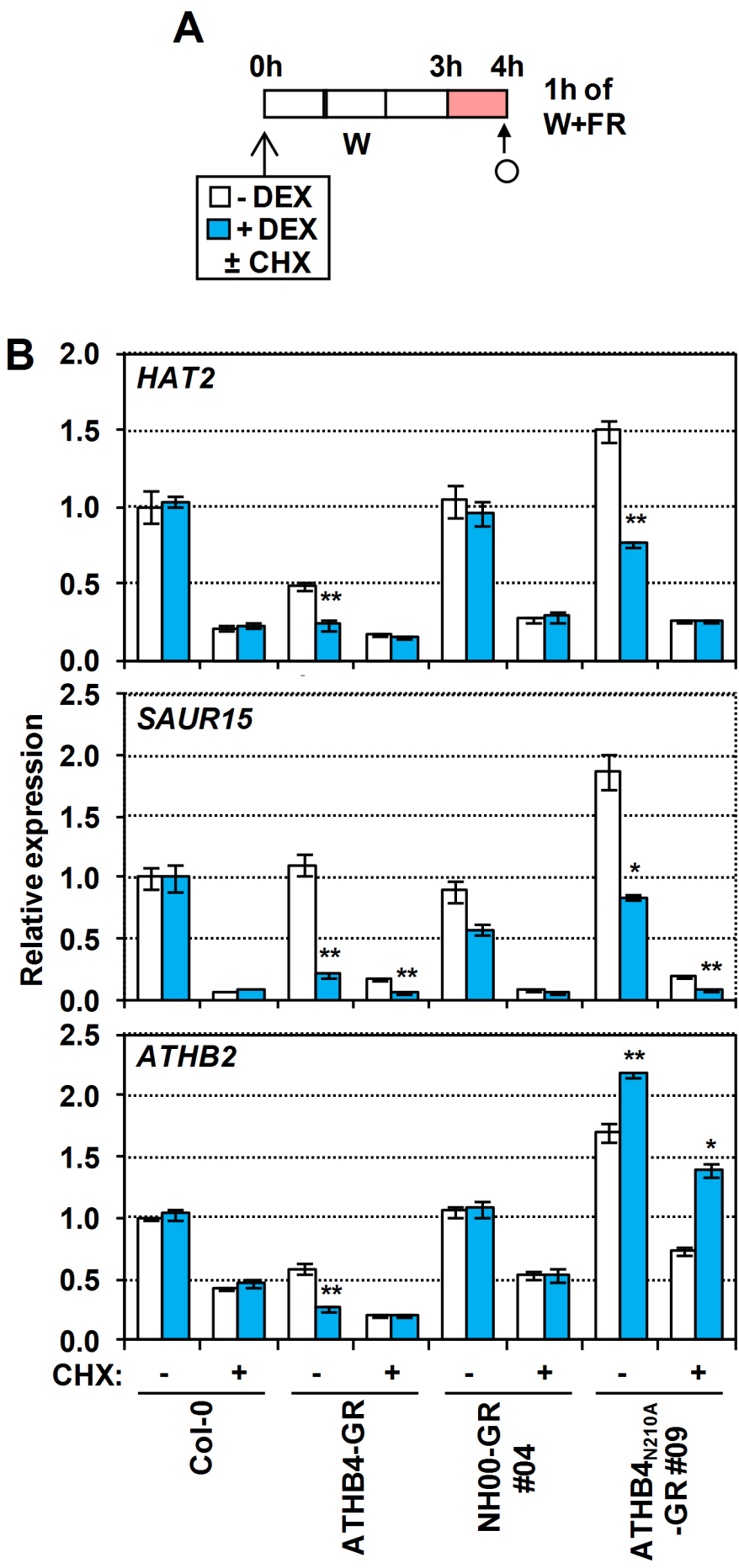
A
0h
3h
4h
1h of
W+FR
W
- DEX
+ DEX
± CHX
B
HAT2
SAUR15
ATHB2
Relative expression
2.0
1.5
1.0
0.5
0.0
2.5
CHX:
-
+
Col-0
ATHB4-GR
NH00-GR
#04
ATHB4N210A
-GR #09

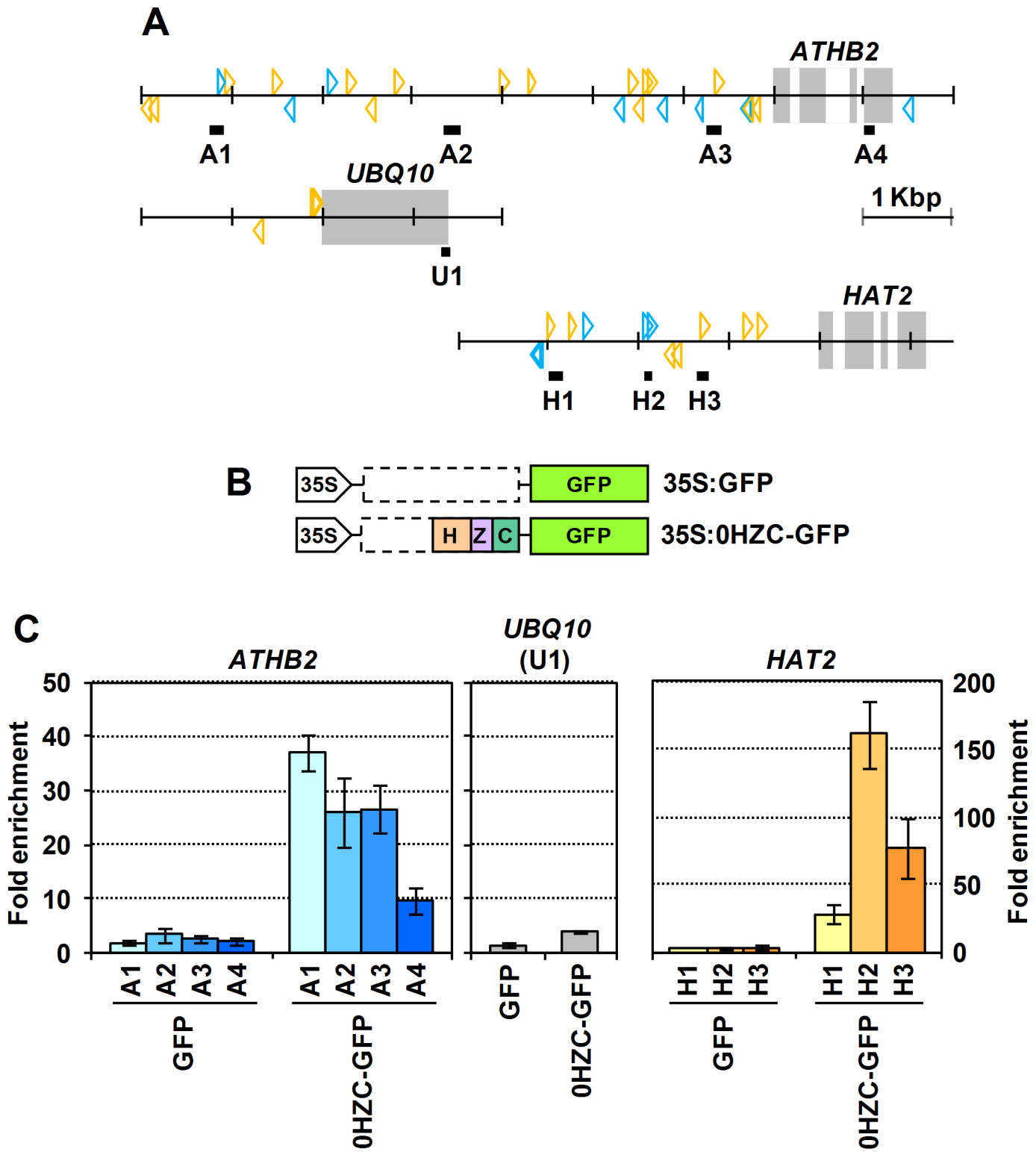
A
ATHB2
A1
A2
A3
A4
UBQ10
1 Kbp
U1
HAT2
H1
H2
H3
B
35S
GFP
35S:GFP
35S
H
Z
C
GFP
35S:0HZC-GFP
C
ATHB2
UBQ10
(U1)
HAT2
Fold enrichment
50
40
30
20
10
0
200
150
100
50
0
A1
A2
A3
A4
GFP
0HZC-GFP
H1
H2
H3

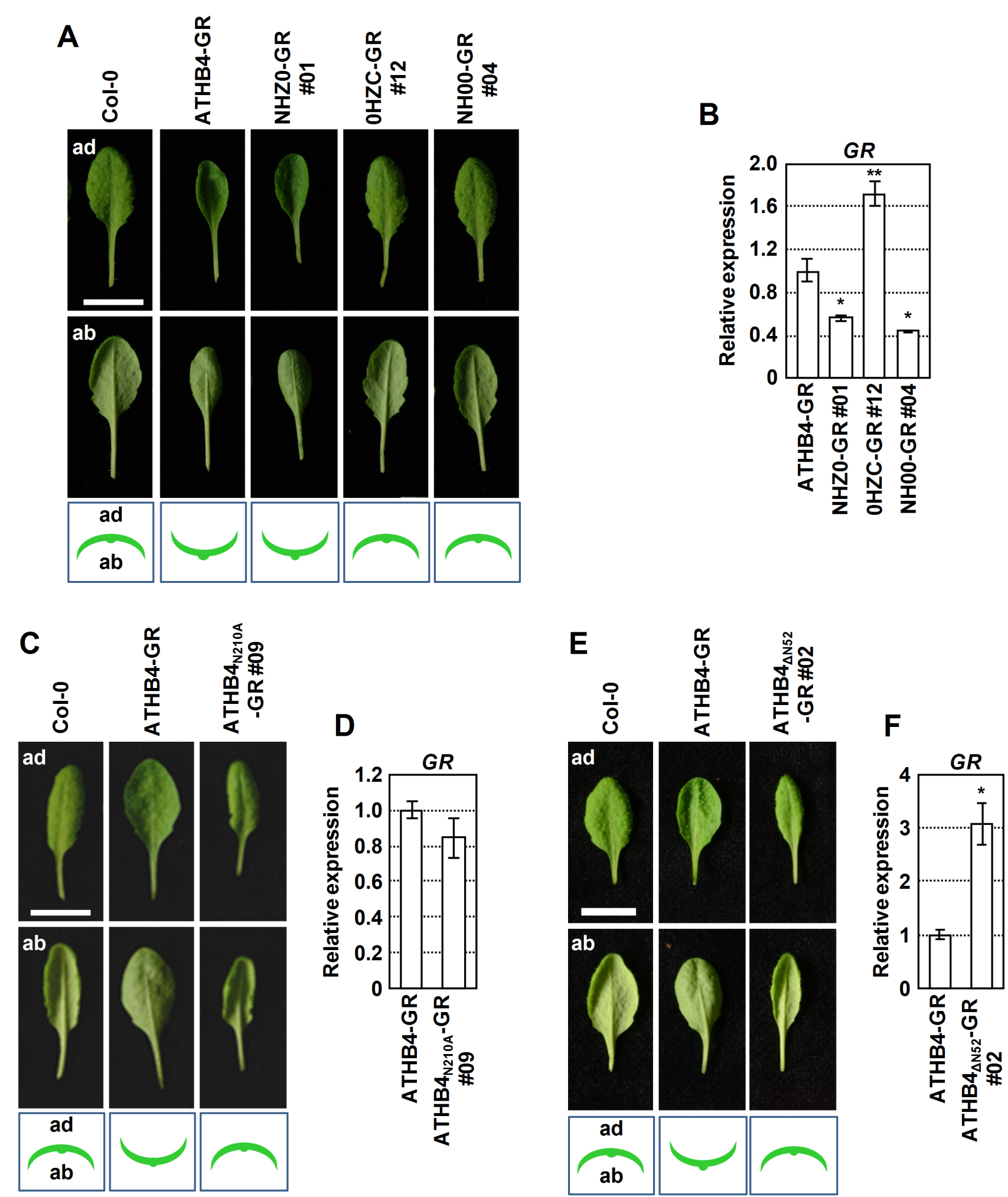
A
Col-0
ATHB4-GR
NHZ0-GR #01
0HZC-GR #12
NH00-GR #04
ad
ab
B
GR
Relative expression
2.0
1.6
1.2
0.8
0.4
0
**
*
*
ATHB4-GR
NHZ0-GR #01
0HZC-GR #12
NH00-GR #04
C
Col-0
ATHB4-GR
ATHB4N210A -GR #09
D
GR
Relative expression
1.2
1.0
0.8
0.6
0.4
0.2
0
ATHB4-GR
ATHB4N210A-GR #09
E
Col-0
ATHB4-GR
ATHB4ΔN52 -GR #02
F
GR
Relative expression
4
3
2
1
0
*
ATHB4-GR
ATHB4ΔN52-GR #02

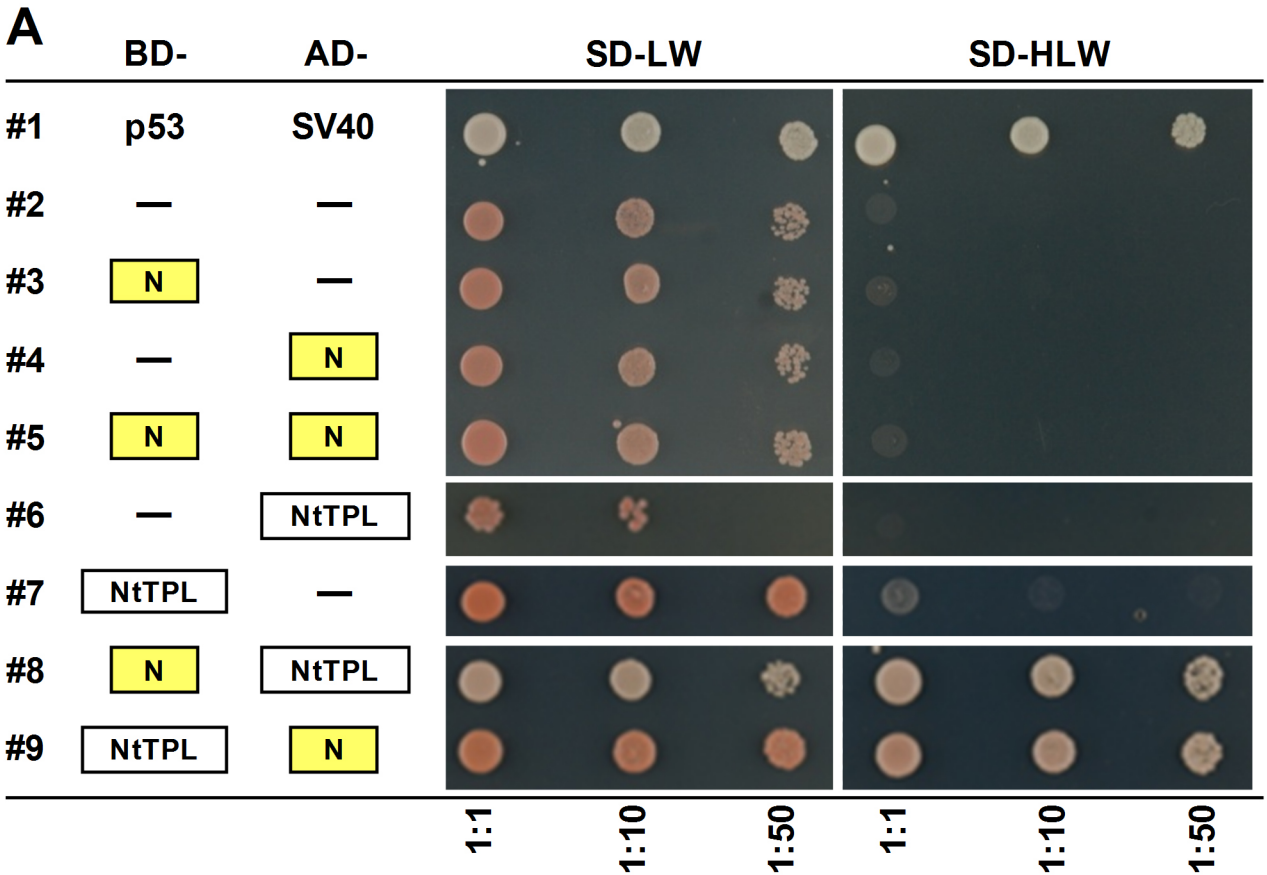
A
BD-
AD-
SD-LW
SD-HLW
#1
p53
SV40
#2
—
—
#3
N
—
#4
—
N
#5
N
N
#6
—
NtTPL
#7
NtTPL
—
#8
N
NtTPL
#9
NtTPL
N
1:1
1:10
1:50
1:1
1:10
1:50

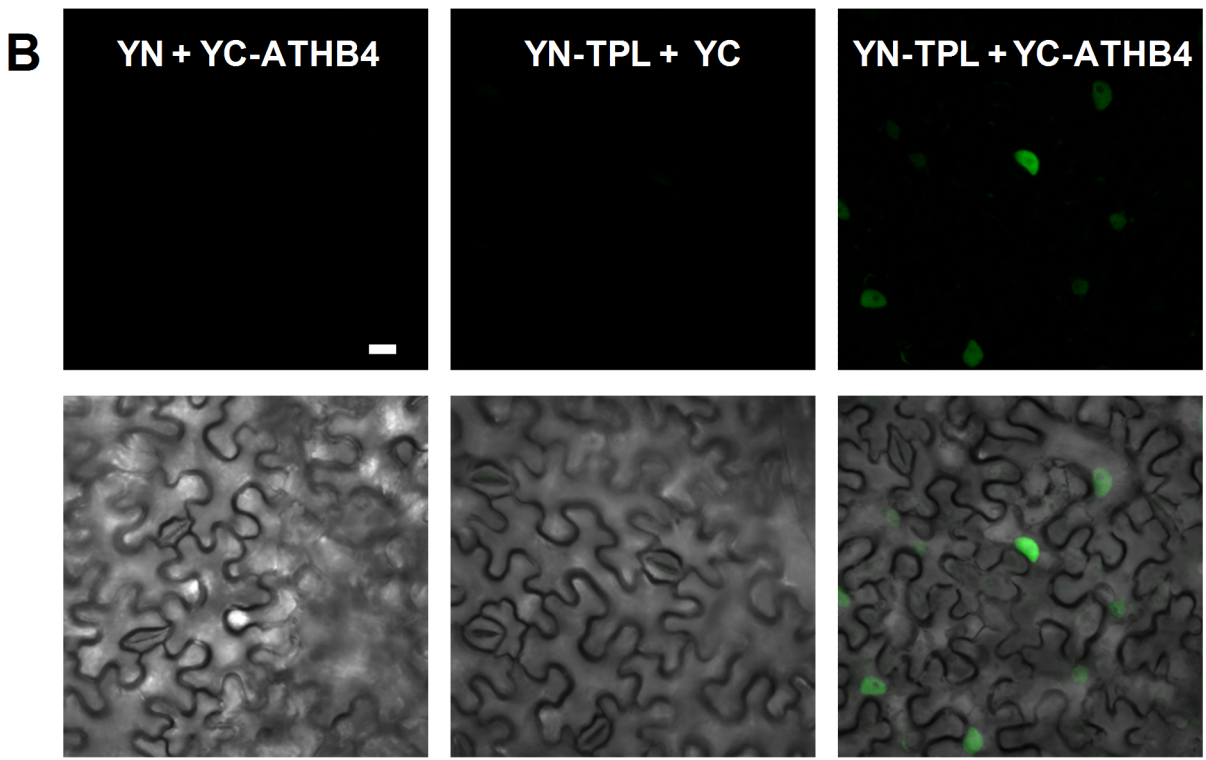
B
YN + YC-ATHB4
YN-TPL + YC
YN-TPL + YC-ATHB4

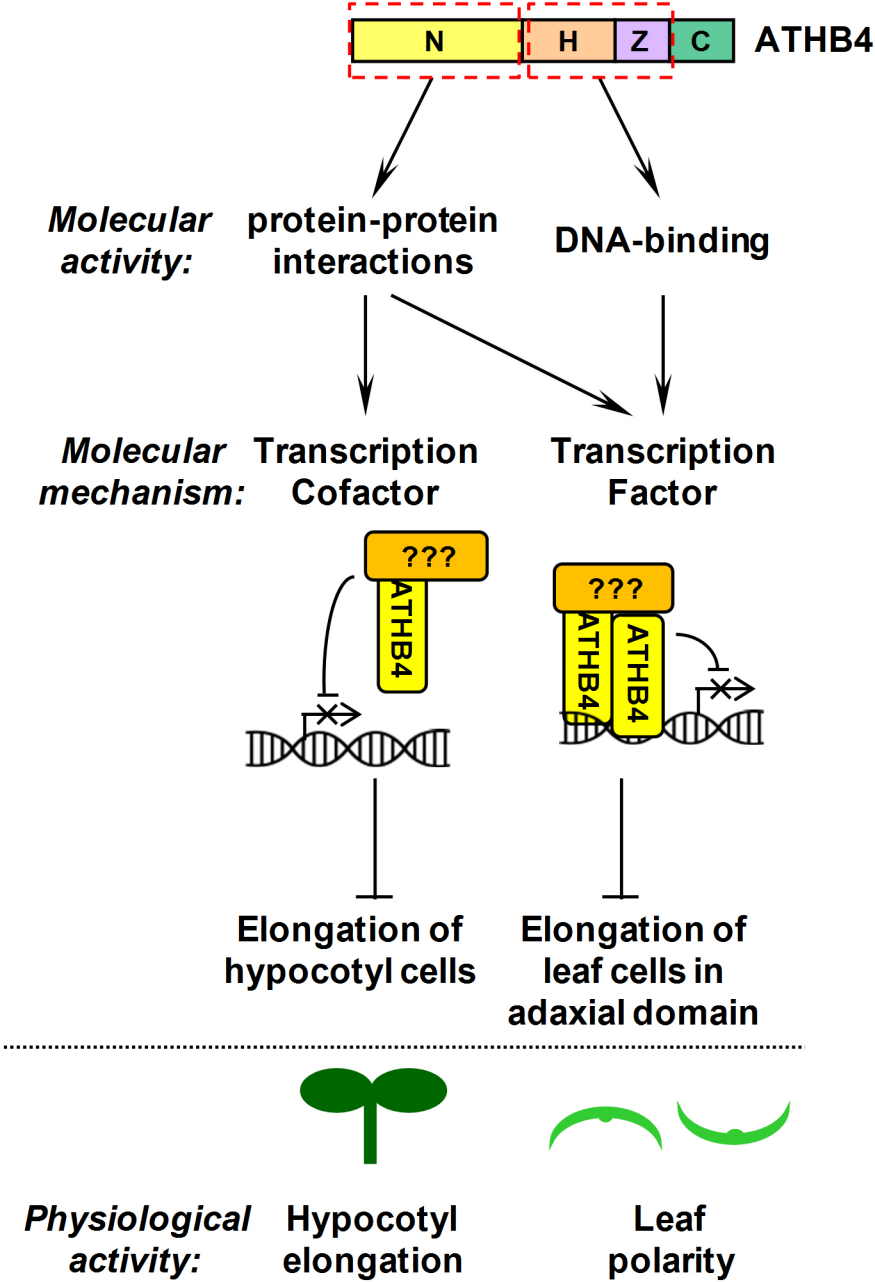
N
H
Z
C
ATHB4
Molecular activity:
protein-protein interactions
DNA-binding
Molecular mechanism:
Transcription Cofactor
Transcription Factor
???
ATHB4
???
ATHB4
ATHB4
Elongation of hypocotyl cells
Elongation of leaf cells in adaxial domain
Physiological activity:
Hypocotyl elongation
Leaf polarity